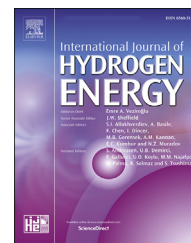


Available online at [www.sciencedirect.com](http://www.sciencedirect.com)

ScienceDirect

journal homepage: [www.elsevier.com/locate/he](http://www.elsevier.com/locate/he)

# A novel process for CO<sub>2</sub> capture from steam methane reformer with molten carbonate fuel cell

Federico d'Amore <sup>a,\*</sup>, Luis M.C. Pereira <sup>b</sup>, Stefano Campanari <sup>a</sup>,  
Matteo Gazzani <sup>c,d</sup>, Matteo C. Romano <sup>a,\*\*</sup>

<sup>a</sup> Politecnico di Milano, Department of Energy, via Lambruschini 4, IT-20156 Milano, Italy

<sup>b</sup> Centre Scientifique & Technique Jean Féger (CSTJF), Av. Larribau, 64000 Pau, France

<sup>c</sup> Copernicus Institute of Sustainable Development, Utrecht University, CS Utrecht, 3584, the Netherlands

<sup>d</sup> Inorganic Membranes and Membrane Reactors, Sustainable Process Engineering, Chemical Engineering and Chemistry, Eindhoven University of Technology, Eindhoven, the Netherlands

## HIGHLIGHTS

- CO<sub>2</sub> capture from steam methane reforming with molten carbonate fuel cell is studied.
- A novel process based on off-gas anode feed and 2-stage cell is proposed.
- Novel process achieves 90–95% CO<sub>2</sub> capture, against 85% natural gas fed anode process.
- Novel process has smaller cell area and H<sub>2</sub> production cost than natural gas feed.
- Novel process has comparable H<sub>2</sub> production cost with conventional MEA CO<sub>2</sub> capture.

## ARTICLE INFO

### Article history:

Received 13 March 2023

Received in revised form

3 June 2023

Accepted 12 June 2023

Available online 27 June 2023

### Keywords:

Steam methane reformer

Molten carbonate fuel cell

Carbon dioxide capture

Process simulation

Techno-economic modelling

## ABSTRACT

Hydrogen (H<sub>2</sub>) production via steam methane reforming is a mature and cost-effective technology. However, carbon capture and storage is required to decrease its carbon dioxide (CO<sub>2</sub>) emissions. The adoption of molten carbonate fuel cells as means to capture CO<sub>2</sub> from flue gases is attracting scientific interest thanks to their inherent thermodynamic advantage of separating CO<sub>2</sub> while producing electricity. This study investigates and benchmarks the performance of an H<sub>2</sub> production plant equipped with molten carbonate fuel cell for post-combustion CO<sub>2</sub> capture, by proposing a novel configuration where the cell anode is fed with the carbon-rich off-gas from the H<sub>2</sub> separation unit. It emerges that the process can achieve higher capture rates than the reference solvent-based plant: 85–90% with single cell, 95% with two-stage cell. Moreover, recycling the carbon-rich off gas to the anode allows for smaller cell area, and potentially lower H<sub>2</sub> production costs compared to the benchmark.

© 2023 Hydrogen Energy Publications LLC. Published by Elsevier Ltd. All rights reserved.

\* Corresponding author.

\*\* Corresponding author.

E-mail addresses: [federico.damore@unipd.it](mailto:federico.damore@unipd.it) (F. d'Amore), [matteo.romano@polimi.it](mailto:matteo.romano@polimi.it) (M.C. Romano).

<https://doi.org/10.1016/j.ijhydene.2023.06.137>

0360-3199/© 2023 Hydrogen Energy Publications LLC. Published by Elsevier Ltd. All rights reserved.

**List of symbols**

AR	annualisation ratio
ASU	air separation unit
ATR	autothermal reforming
CAPEX	capital cost
CCA	cost of CO <sub>2</sub> avoided
CCR	carbon capture rate
CCS	carbon capture and storage
CFP	coal-fired plant
CHP	combined heat and power
CPU	low-temperature phase-change purification unit
EPC	engineering and procurement cost
FTR	fired tubular reformer
GHG	greenhouse gas
h	heat transfer coefficient
HP	high pressure
HRSG	heat recovery steam generator
ICE	internal combustion engine
IGCC	integrated gasification combined cycle
LP	low pressure
MCFC	molten carbonate fuel cell
MEA	monoethanolamine
NG	natural gas
NGCC	natural gas combined cycle
NGF	natural gas feed plant
OGF	off-gas feed plant
OGF-2	off-gas feed 2-stage cell plant
OGF-2-Deg	off-gas feed 2-stage cell plant with effect of cell degradation
OPEX	operative expenditures
OSBL	off-site costs
PSA	pressure swing adsorption
SMR	steam methane reformer
SPECCA	specific primary energy consumption for unit of CO <sub>2</sub> avoided
TDPC	total direct plant cost
TPC	total plant cost
UF	fuel utilisation factor
WGS	water-gas shift

**Introduction**

Hydrogen (H<sub>2</sub>) may become a crucial player in the decarbonisation challenge, by contributing to the reduction of greenhouse gases emissions (GHGs) in a multitude of sectors and markets (e.g., power, high temperature heat, hard-to-electrify transportation, industry) beyond its current use [1]. In particular, the blue H<sub>2</sub> route (i.e., H<sub>2</sub> production from a fossil fuel coupled with carbon capture and storage - CCS) may be preferable for large-scale production over electrolytic H<sub>2</sub> until the electric grid is largely decarbonised, provided that low carbon dioxide (CO<sub>2</sub>) emissions are achieved and that it relies on low-leakage natural gas (NG) supply chains [2,3]. Moreover, blue H<sub>2</sub> may play an important role in the short-term abatement of GHGs emissions from refineries [4,5], which are responsible for roughly one tenth of worldwide industrial GHGs [6].

Blue H<sub>2</sub> can be produced from NG reforming, typically through steam methane reforming (SMR) or autothermal reforming (ATR). Due to the limited methane conversion, which is mainly given by the limit in the achievable reforming temperature, a capture efficiency above 90% with conventional SMR technology can only be obtained via post-combustion CO<sub>2</sub> capture technologies [7,8]. As an alternative, the electrification of heat demand of SMRs would offer the possibility to (partially) decarbonise these units and provide heat at higher flexibility and compactness [9,10], but this option avoids only those CO<sub>2</sub> emissions deriving from fuel combustion.

Molten carbonate fuel cells (MCFCs) are electrochemical devices that can separate CO<sub>2</sub> at high temperature from gas mixtures containing CO<sub>2</sub> and O<sub>2</sub> (such as combustion flue gases), while oxidising a gaseous fuel and producing electricity [11]. MCFCs have been assessed in several conceptual studies as post-combustion capture systems; the common conclusion is that MCFCs show potentially superior performance (certainly thermodynamic, but also cost-wise), with respect to solvents in different applications, such as power plants [12–14], cement plants [15], iron and steel plants [16], H<sub>2</sub> plants [17], and marine transportation [18] (Table 1). Nevertheless, despite the preparatory work for technology validation, including a FEED study [19], demonstration of MCFC-based CO<sub>2</sub> capture systems at scale has not been documented, yet. In the case of blue H<sub>2</sub> production, MCFC-based CO<sub>2</sub> capture represents an attractive alternative to conventional processes, given the potential co-production of electricity, blue H<sub>2</sub>, and steam (i.e., useful products for the refinery itself), besides CO<sub>2</sub> separation [20,21].

A novel concept for the use of MCFCs as CO<sub>2</sub> capture and H<sub>2</sub> production devices has been recently proposed by Consonni et al. [17] and Barckholtz et al. [21]. The overarching idea is to operate the MCFC with low fuel utilisation factor (UF), by exploiting the fuel cell anode as a steam methane reformer/partial oxidiser of the NG feed. Consonni et al. [17] investigated the integration of such MCFC system in an SMR plant. The maximum H<sub>2</sub> production was obtained with a fuel UF of 45%, leading to an increase in the H<sub>2</sub> output by up to +37% compared to the existing SMR and to a reduction in specific CO<sub>2</sub> emissions by more than 95% (from 8.7 kg of CO<sub>2</sub>/kg of H<sub>2</sub> to 0.44 kg of CO<sub>2</sub>/kg of H<sub>2</sub>). Barckholtz et al. [21] assessed the same concept by treating the flue gas of an NG combined cycle based on a 200 MW gas turbine. The maximum H<sub>2</sub> production (almost 300 MW<sub>LHV</sub> of H<sub>2</sub>) was achieved for a fuel UF equal to 30% and for a CO<sub>2</sub> capture rate of 90%.

This study investigates the application of MCFCs as CO<sub>2</sub> capture devices from the flue gas of an SMR plant based on a fired tubular reformer (FTR); differently from Refs. [17,21], this study does not aim at increasing the production of H<sub>2</sub> via adopting MCFCs, but rather at reducing the CO<sub>2</sub> emissions of the H<sub>2</sub> production process, while keeping the H<sub>2</sub> output constant. The objective of this study is to evaluate the techno-economic performance of an integrated SMR-MCFC blue H<sub>2</sub> plant, in comparison with a benchmark SMR plant with conventional amine-based post-combustion CO<sub>2</sub> capture. The novelty of this work lies in the combination of the following original points:

**Table 1 – Studies on MCFC CO<sub>2</sub> capture. CCR, carbon capture rate; CFP, coal-fired plant; CHP, combined heat and power; HRSG, heat recovery steam generator; IGCC, integrated gasification combined cycle; ICE, internal combustion engine; NGCC, natural gas combined cycle. Anode feed: NG/CH<sub>4</sub> (unless stated).**

Case study	MCFC		CO <sub>2</sub> abatement		Reference
	Voltage	Power out.	CCR	CCA <sup>a</sup>	
	[V]	[MW <sub>el</sub> ]	[0.%]	[€/t CO <sub>2</sub> ]	
CFP	0.76	198	0.77	–	[22]
CFP	0.5–0.75	95	0.3–0.99	–	[23]
CFP	0.4–0.5	0.0027–0.0032 <sup>b</sup>	0.52–0.74	–	[24]
CFP	0.67–0.71	251–314	0.71–0.88	55	[25]
CFP	0.7	100	0.58	40	[26]
CFP	0.7	124	0.83	29	[27]
CFP	0.76	337	0.76	25–39	[13]
CFP	0.71	95–150	<0.9	13–63	[28]
CFP	0.69	7	0.9	–	[29]
GT	–	2	0.37	–	[30]
GT	0.5–0.7	<1	0.55	–	[31]
GT	0.49	14	0.91	–	[32]
GT	0.74–0.81	0.0025–0.0032	–	–	[33]
GT	0.74–0.81	1.1–2.8	0.0–0.9	–	[34]
GT	0.7–0.73	16–20	0.70	–	[35]
NGCC	0.7	89	0.80	–	[36]
NGCC	0.68–0.71	102–111	0.76–0.85	–	[12]
NGCC	0.75	<28/84	0.74/0.54	–	[37]
NGCC	0.7–0.75	81	0.75	–	[38]
NGCC	0.7–0.75	81–120	0.73–0.76	–	[39]
NGCC	–	133	0.58	28–45	[40]
NGCC	0.71	95	0.72	120.4	[41]
NGCC	0.72	23	0.85	–	[42]
NGCC	0.7–0.9	51–95	0.45–0.85	82	[43]
NGCC	0.72	225	0.82	33–44	[13]
NGCC	0.7	181–201	0.80–0.81	43–67	[44]
NGCC	0.65	19–145	>0.90	–	[21]
IGCC	0.57–0.71	106/144	0.59/0.91	–	[45]
IGCC	0.65–0.7	98	0.88	58	[46]
ICE	0.5–0.7	<1	0.55	–	[31]
CHP	0.71	0.386	0.62	–	[47]
ICE <sup>c</sup>	63–0.67	0.193–0.710	0.20–0.80	–	[48]
Cement	0.7–0.8	69–106	0.56–0.76	–	[15]
Boiler	–	76	0.90	–	[49]
Steel	0.67–0.79	82–433	0.91–0.95	23–55	[16]
SMR	0.65–0.79	61–74	0.95	–	[17]

<sup>a</sup> Costs in \$ converted via average \$/€ rate (referred to year of publication).

<sup>b</sup> Per cubic metre of flue gas at normal conditions.

<sup>c</sup> Anode fed with NG and biogas.

- A novel MCFC configuration is here investigated, which exploits part of the off-gas deriving from the SMR H<sub>2</sub> purification unit as fuel to the MCFC, instead of NG (Table 1 shows that previous studies focussed on NG as fuel to the MCFC). As the results will show, this novel configuration has the potential of reducing the MCFC size for a given CO<sub>2</sub> capture rate, with major beneficial effects on costs and economic performance indicators.
- Building upon the performance of the novel off-gas feed configuration and on the work of Spinelli et al. [15], this study assesses how a multi-stage cell configuration with inter-cooling would further improve the process.
- This study proposes an off-design calculation procedure that can help providing insights into the effect of cell

degradation on the mass and energy balances of the plant and, ultimately, on costs.

## Plants description

The analyses were conducted on greenfield plants and based on the following case studies:

- SMR (Fig. 1a): reference standalone FTR without CO<sub>2</sub> capture, designed to produce 100000 Nm<sup>3</sup>/h of H<sub>2</sub> (corresponding to 299.5 MW<sub>LHV</sub>), comprising high temperature water-gas shift (WGS), pressure swing adsorption (PSA), steam cycle (set at 485 °C at 100 bar), and low pressure (LP)

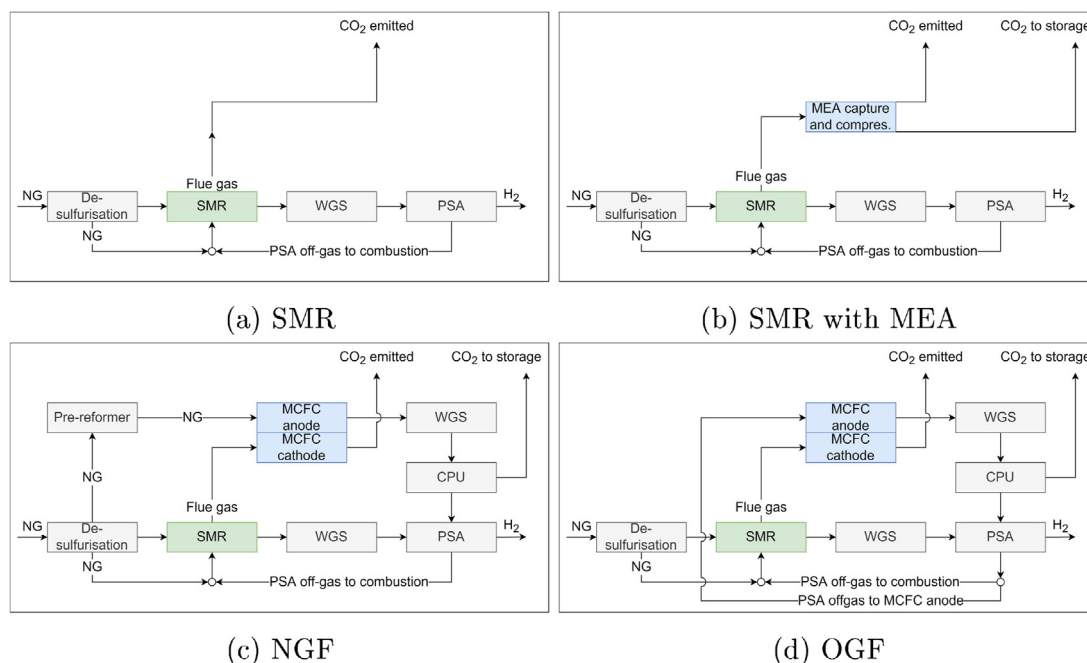


**Fig. 1** – Simplified plant schemes for: (a) SMR, (b) SMR with MEA, (c) NGF, and (d) OGF configurations.

steam export (at 6 bar). This plant is characterised by an NG-to-H<sub>2</sub> efficiency of 73.5% and specific CO<sub>2</sub> emissions of 9.29 kg of CO<sub>2</sub>/kg of H<sub>2</sub>, being the net electric and thermal power outputs equal to 10.4 MW<sub>el</sub> and 23.2 MW<sub>th</sub>, respectively. The detailed plant description is reported in the Supplementary Material.

- **SMR with MEA (Fig. 1b)**: SMR with post-combustion CO<sub>2</sub> capture with monoethanolamine (MEA), designed for a CO<sub>2</sub> capture rate of 90% and a specific heat demand of 3.57 MJ<sub>th</sub>/kg of captured CO<sub>2</sub> [7]. This plant is considered as benchmark case for performance and costs comparison with MCFC-based CO<sub>2</sub> capture. The SMR plant flowsheet is modified to maximise the LP steam generation to be used for solvent regeneration, to avoid an increase in NG consumption upon operation of the MEA-based CO<sub>2</sub> capture plant. This is done by eliminating the steam turbines and the high pressure (HP) evaporation level, by keeping the medium pressure (MP) evaporation level needed for the pre-reformer charge, by exploiting the LP evaporation level to generate steam, and by adding an ammonia-based heat pump to exploit the heat content in the syngas to generate additional LP steam for solvent regeneration purposes. As a result, the NG-to-H<sub>2</sub> efficiency is unchanged with respect to the SMR without CO<sub>2</sub> capture, whereas the specific CO<sub>2</sub> emissions decrease from 9.29 to 0.93 kg of CO<sub>2</sub>/kg of H<sub>2</sub>. The detailed plant description is reported in the Supplementary Material.
- **SMR with NG fed (NGF) MCFC (Fig. 1c)**: NG-based MCFC. The SMR flue gases are sent to the MCFC cathode for CO<sub>2</sub> separation. A CO<sub>2</sub> lean stream is produced at the cathode residue and emitted to the atmosphere. The MCFC anode is fed with pre-reformed NG. The anode residue is sent to a WGS converter. The shifted syngas stream is sent to the low-temperature phase-change purification unit (CPU) to

produce a high-purity CO<sub>2</sub> stream and a flow rate that is recycled to the PSA unit downstream the SMR.

- **SMR with PSA off-gas fed (OGF) MCFC (Fig. 1d)**: off-gas-based MCFC. Differently from the NGF case, the MCFC anode is fed with PSA off-gas. Since the PSA off-gas has higher carbon intensity with respect to NG (0.220 kg of CO<sub>2</sub>/MJ<sub>LHV</sub>, against 0.057 kg of CO<sub>2</sub>/MJ<sub>LHV</sub>), this configuration keeps the carbon-rich fuel on the MCFC anode side and reduces the flow rate of CO<sub>2</sub> in the SMR to be separated by the MCFC (therefore, its area) for a given overall CO<sub>2</sub> capture rate. Thanks to the lack of higher hydrocarbons in the off-gas fuel, this configuration also allows simplifying the plant flowsheet by eliminating the pre-reformer upstream the cell anode (conversely, a pre-reformer is needed in the NGF case). Based on the OGF case, the following sub-cases are analysed as well:
  - OGF-2: involving the adoption of two cells in series with inter-cooling to decrease the air dilution at the cathode inlet and enhance the CO<sub>2</sub> separation efficiency for a given cell potential.
  - OGF-2-Deg: equivalent to the OGF-2 case, but including the effect of cell degradation on the overall performance of the system.

#### NGF case: CO<sub>2</sub> capture with NG-fed MCFC

The MCFC integration requires some modifications to the standalone SMR scheme (Fig. 2). The main changes are the addition of an MCFC system followed by a CPU, to generate a high purity CO<sub>2</sub> stream [Fig. 2, stream CPU-22].

This study assumes a greenfield design approach, that entails the choice of feeding the SMR flue gases to the cell cathode [stream 22] at high temperature to comply with the MCFC design inlet temperature of 575 °C. As a result, the preheating

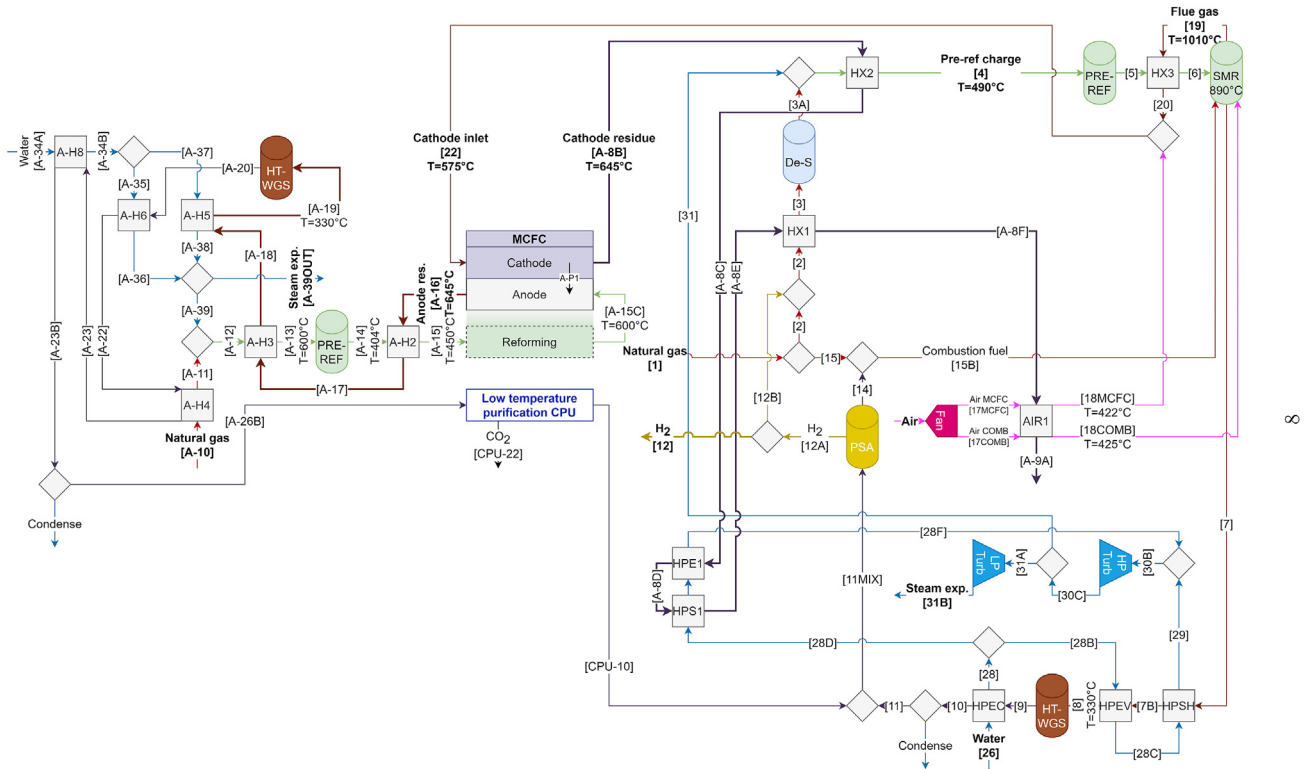


**Fig. 2 – Plant flowsheet of the integrated MCFC SMR, case study NGF. Streams properties and compositions in Supplementary Material.**

requirements in the SMR section are now largely fulfilled by the hot cathode off-gas rather than by the hot flue gases of the SMR furnace. The distinctive element of this case study (natural gas feed: NGF case) is represented by the choice of feeding the cell anode with additional NG [stream A-14], as proposed in conventional MCFC-based plants. The MCFC unit consists of an anode, a cathode, and a reforming section upstream the anode; a pre-reformer (upstream the MCFC) and a WGS section (downstream the MCFC) complete the overall separation system, as shown in Fig. 2. The flue gases deriving from the combustion in the SMR section are sent to the MCFC cathode, while the anode feed is NG. The flue gases deriving from the SMR furnace (74 kg/s) [stream 20] are firstly mixed with air (264 kg/s) [stream 18MCFC]. The pre-heating temperature of air is determined to obtain 575 °C after mixing with the flue gases [stream 22]. Then, the mixture of flue gases and air is sent to the MCFC cathode. The air flow rate is determined via the heat balance of the MCFC to keep the cell outlet temperature at its design value (645 °C). This operation and design decision is taken to guarantee that the MCFC operates according to the product characteristics, where temperature profiles are key for integrity.

The amount of CO<sub>2</sub> permeating from the cathode to the anode is set to obtain a CO<sub>2</sub> molar fraction in the cathode exhaust gas equal to 1%<sup>mol</sup>, as suggested by Consonni et al. [17]; this is done to avoid the formation of hydroxide ions in the cathode that may be transported to the anode, which may occur at very low CO<sub>2</sub> concentrations [14]. At the cell anode exit, after heat recovery, the cold cathode exhaust [stream A-9A] is vented to the atmosphere at 1.01 bar and 168 °C. The NG feed to the anode (3.46 kg/s) [stream A-10] is heated up to 600 °C

and sent to the adiabatic pre-reformer [stream A-13], that operates at 4 bar with a steam to carbon ratio equal to 2.1. The target steam to carbon ratio is obtained by mixing 7.73 kg/s of LP steam [stream A-39]. The pre-reformed stream [stream A-14] exits at 404 °C, heated up again to 450 °C and fed to the MCFC, where it mixes with the CO<sub>2</sub>, H<sub>2</sub>O, and O<sub>2</sub> permeating from the cathode to the anode, to produce the anode off-gas at 645 °C [stream A-16]. The hot anode exhaust gas is cooled down by generating LP steam and by pre-heating the NG, the pre-reformer charge, and the reformer charge. Finally, the anode exhaust gas is further cooled down to ambient temperature to condense water and sent to the CPU [stream A-26B].

The CPU (Fig. 3) delivers high purity CO<sub>2</sub> (99%<sup>mol</sup>) while recovering unconverted H<sub>2</sub> and CO [CPU-10]. In particular, the cold anode residue [stream A-26B] undergoes a first compression [block inter-comp1], modelled as a 4-stage compressor with inter-cooling with fixed discharge pressure of 32 bar. The resulting stream [stream CPU-2] is then treated in a two-stage phase separation process constituted by 2 CO<sub>2</sub> separation drums, 2 expansion valves and 2 heat exchangers. The resulting streams are: (i) a CO<sub>2</sub>-depleted residue [stream CPU-10] that is sent to the PSA unit of the SMR for H<sub>2</sub> recovery; and (ii) two high-purity CO<sub>2</sub> streams for the separators [streams CPU-18, CPU14–B] which are mixed (at 15 bar) and compressed through a 2-stage inter-cooled compressor with fixed discharge pressure of 100 bar. Then, the CO<sub>2</sub>-rich stream is cooled down to ambient temperature and pumped out at 150 bar. The result is a high purity (99%<sup>mol</sup> of CO<sub>2</sub>), supercritical CO<sub>2</sub> stream (150 bar, 24.93 kg/s) [stream CPU-22], ready for permanent geological storage.





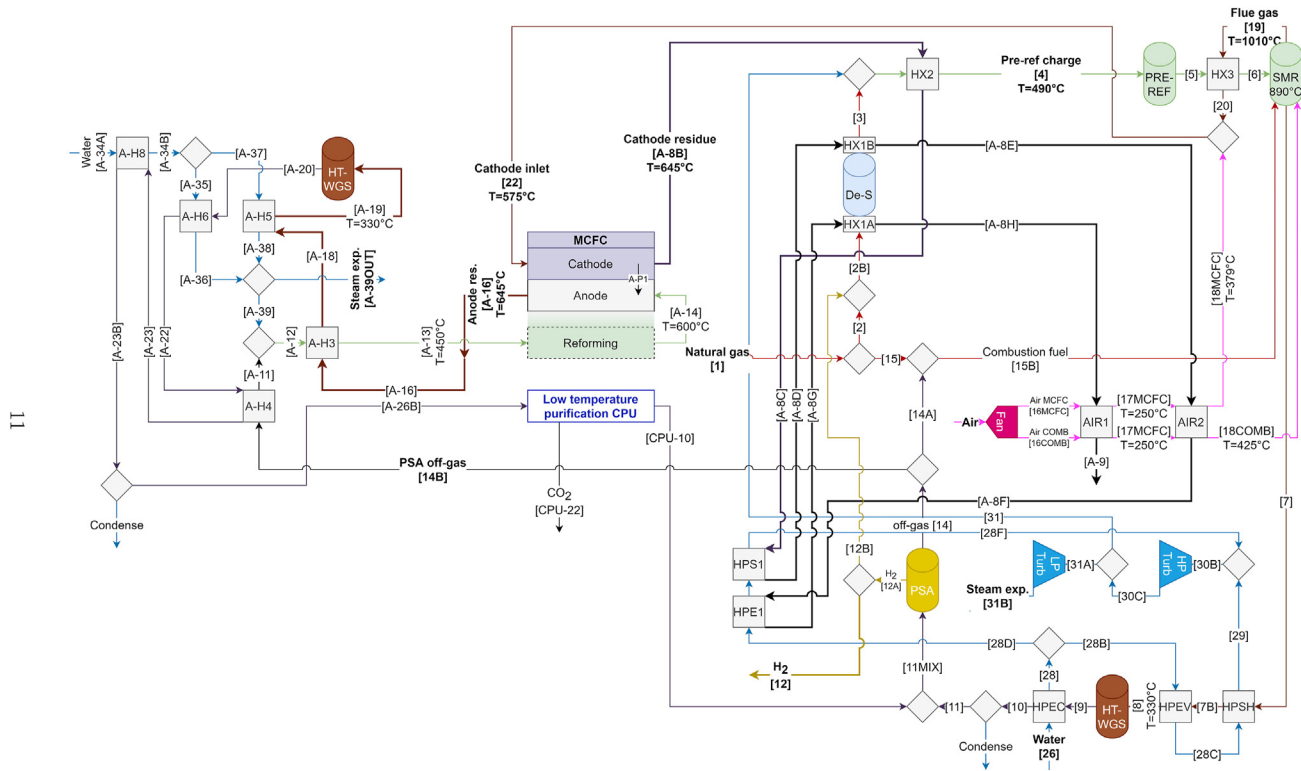


**Fig. 4 – Plant flowsheet of the integrated MCFC SMR, case study OGF. Streams properties and compositions in Supplementary Material.**

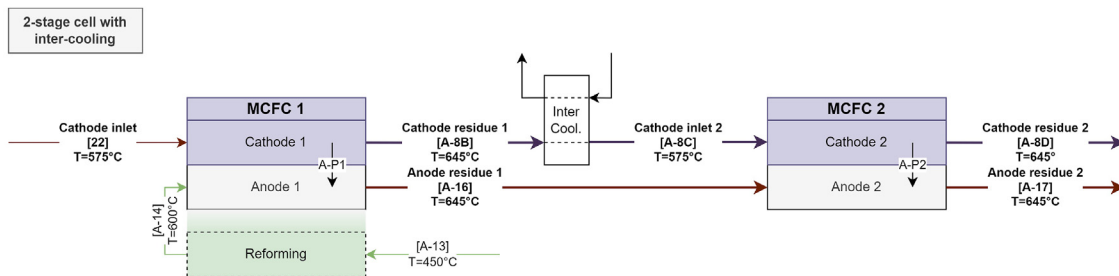


**Fig. 5 – Flowsheet of the 2-stage MCFC cell configuration with inter-cooling, case study OGF-2. Streams properties and compositions in Supplementary Material.**

the carbonate ions  $\text{CO}_3^-$  and the total current density  $j_{\text{TOT}}$  [A/m<sup>2</sup>]:

$$t_{\text{CO}_3^-} = \frac{j_{\text{CO}_3^-}}{j_{\text{TOT}}} \quad (2)$$

being  $j_{\text{CO}_3^-}$  and  $j_{\text{TOT}}$  in Eq. (2) defined by Eqs.(3) and (4), where  $F$  is the Faraday constant and  $n_{\text{CO}_3^-}$  [mol/s] and  $n_{\text{OH}^-}$  [mol/s] are the molar flow rates of  $\text{CO}_3^-$  and  $\text{OH}^-$ , respectively, through the electrolyte:

$$j_{\text{CO}_3^-} = \frac{2Fn_{\text{CO}_3^-}}{A_{\text{cell}}} \quad (3)$$

$$j_{\text{TOT}} = \frac{F(2n_{\text{CO}_3^-} + n_{\text{OH}^-})}{A_{\text{cell}}} \quad (4)$$

The carbonate transference number  $t_{\text{CO}_3^-}$  depends on the concentrations of  $\text{CO}_2$  and  $\text{H}_2\text{O}$  [50–52]. High  $\text{CO}_2$

concentrations result in higher  $t_{\text{CO}_3^-}$ , with limited effects of  $\text{H}_2\text{O}$  on  $j_{\text{TOT}}$ . Oppositely, an increase in  $\text{H}_2\text{O}$  concentration leads to a reduction of  $t_{\text{CO}_3^-}$ . This study assumes a constant value of transference number  $t_{\text{CO}_3^-}$  equal to 0.75 (in line with Audasso et al. [50]), involving that 1 mol of  $\text{H}_2\text{O}$  permeates every 3 mol of  $\text{CO}_2$ .

The case study designed to include the effect of cell degradation (OGF-2-Deg) is implemented by assuming a downward shift in the polarisation curve equal to 5% of the nominal potential (i.e., as suggested by Morita et al. [53]), by considering the same cells surface area of OGF-2 and by adjusting the cell potential (and therefore the current density and UF), so that the target MCFC outlet temperature is kept constant (i.e., 645 °C). In OGF-2-Deg, the NG and PSA off-gas flow rates to the SMR burners are kept constant, so as not to modify the fuel mix and the flue gas flow rate and composition. Similarly, also the air inlet to the cell is kept the same as

**Table 2 – Summary of the main input data (details in the Supplementary Material).**

Plant	Component	Parameter	Value	Unit
SMR	Pre-reformer	Steam to carbon ratio	3.4	mol/mol
	Reformer	Outlet temperature	890	°C
	PSA	Hydrogen recovery	90	%
	LP steam	Pressure	6	bar
	HP steam	Pressure/temperature	100/485	bar/°C
MEA	CO <sub>2</sub> separation	CO <sub>2</sub> separation efficiency	90	%
	CO <sub>2</sub> separation	Reboiler duty	3.57	GJ/t CO <sub>2</sub>
MCFC	Cathode	Inlet temperature	575	°C
	Cathode	Outlet temperature	645	°C
	Cathode	CO <sub>2</sub> concentration in cathode exhaust	1	% <sup>mol</sup>
	Pre-reformer	Inlet temperature	600	°C
	Pre-reformer	Steam to carbon ratio	2.1	—
	Anode	Inlet temperature	600	°C
	Anode	Outlet temperature	645	°C
	Cell	UF	65–75	%
	Cell	Voltage	0.6–0.7	V

in OGF-2. Once a shift in the polarisation curve is imposed, the cell potential is adjusted so that the outlet temperature of the cell is kept constant and equal to the design temperature. This procedure is applied to both MCFCs, leading to variations in UF and CO<sub>2</sub> separation.

### Economic assumptions

An economic analysis was carried out for the investigated case studies to determine their capital costs (CAPEX), operating costs (OPEX), H<sub>2</sub> production costs, and costs of CO<sub>2</sub> avoidance. The economic assessment was performed according to the following assumptions:

- The plants have equivalent operating hours of 8400 h/year. The chosen annualisation ratio is  $AR = 8.67\%/year$  (compatible with IEAGHG [7]). Costs are expressed in €<sup>2018</sup> and updated with CEPCI indexes [54], when needed.
- Nominal values of unitary costs/prices are: NG at 6 €/GJ, electricity at 60 €/MWh (both import and export), and steam export at 24.8 €/MWh. The unitary price of steam is determined by comparison with its production via burning NG (6 €/GJ) with an efficiency of 90%; hence, 24.8 €/MWh. The response of the model upon variations of these costs/prices is tested through sensitivity analyses.
- Costs associated to CO<sub>2</sub> transport and storage stages downstream the modelled processes are assumed equal to 20 €/t of CO<sub>2</sub>. The response of the model upon variations of this cost is tested through a sensitivity analysis.
- Baseline cases are analysed by considering a carbon tax of 100 €/t of CO<sub>2</sub> emitted, the value of which is varied through a sensitivity analysis.

Material and installation costs to determine the CAPEX of the plant are derived from different literature sources [7,16,55–60], and the procedure is summarised in the Supplementary Material. As for the MCFC, its cost is based on the power density of the DFC3000 unit in carbon capture operation mode of 683.8 W/m<sup>2</sup> [20] and on the assumption of 1200 €/kW, which is a perspective cost for large scale production

[13], in line with FuelCell Energy [19]; thus, 820 €/m<sup>2</sup> (the results of a sensitivity analysis will be presented on the value of the latter parameter). As a consequence of the degradation of the cell, this study assumes a MCFC stack replacement occurring every 5 years at the same nominal cost of the initial investment (a sensitivity analysis will be performed on this replacement time). The full recursive replacement of the MCFC is a conservative assumption, since the components for the balance of plant (e.g., vessels, insulation, electric parts) would not degrade at the same rate of the MCFC functional parts.

Material and installation costs are summed up to obtain the total direct plant cost (TDPC). Depending on the level of technology readiness, engineering and procurement costs are defined as 20% (for SMR and SMR with MEA) and 30% (for MCFC-based configurations) of material costs. OSBL costs are given by the 75% of the sum of TDPC and engineering and procurement costs. The total EPC cost is then given by the sum of OSBL, TDPC and engineering and procurement costs. Accordingly, contingency costs are evaluated as 20% of EPC, while owner costs as 15% of EPC, giving the total plant cost TPC (i.e., CAPEX) which is the sum of EPC, contingency and owner costs.

### Key performance indicators

Key performance indicators (KPIs) were defined to compare the different case studies, namely the H<sub>2</sub> production efficiency (i.e.,  $\eta_{H_2}$  [%]), the equivalent H<sub>2</sub> production efficiency (i.e.,  $\eta_{H_2,eq}$  [%]), the carbon capture rate (i.e., CCR [%]), and the specific primary energy consumption per unit of CO<sub>2</sub> avoided (i.e., SPECCA [MJ/kg]).

Both  $\eta_{H_2}$  and CCR evaluate the direct performance of the plant (in terms of H<sub>2</sub> production and CO<sub>2</sub> capture) without considering the effect of indirect fuel consumption and emissions, and are defined as:

$$\eta_{H_2} = \frac{\dot{m}_{H_2} LHV_{H_2}}{\dot{m}_{NG} LHV_{NG}} \quad (5)$$



$$CCR = \frac{\dot{m}_{CO_2, storage}}{\dot{m}_{CO_2, storage} + \dot{m}_{CO_2, emission}} \quad (6)$$

where  $\dot{m}_{H_2}$  [kg/s],  $\dot{m}_{NG}$  [kg/s] and  $\dot{m}_{CO_2}$  [kg/s] are the mass flow rates of  $H_2$ , NG and  $CO_2$ , respectively, while  $LHV_{H_2}$  [119.91 MJ/kg] and  $LHV_{NG}$  [46.498 MJ/kg] are the LHVs of  $H_2$  and NG. In particular, the CCR in Eq. (6) represents the  $CO_2$  capture efficiency; hence, it measures the amount of carbon that is effectively captured (and sent to geological storage) with respect to the total carbon inlet to the plant.

Equivalent  $CO_2$  emissions  $\dot{m}_{CO_2, eq}$  [kg/s] can be evaluated for the cases with  $CO_2$  capture ( $\dot{m}_{CO_2, eq}^{capt}$  [kg/s]) and for that without  $CO_2$  capture ( $\dot{m}_{CO_2, eq}^{no\ capt}$  [kg/s]), and they are defined as the emitted  $CO_2$  flow  $\dot{m}_{CO_2, emission}$  decreased by the indirect emissions avoided as a result of the co-production of electricity  $W_{el}$  and heat  $Q_{th}$  (calculated through the carbon intensities  $\epsilon_{el}$  and  $\epsilon_{th}$  reported in Table 3):

$$\dot{m}_{CO_2, eq} = \dot{m}_{CO_2, emission} - Q_{th}\epsilon_{th} - W_{el}\epsilon_{el} \quad (7)$$

From equivalent  $CO_2$  emissions  $\dot{m}_{CO_2, eq}$  of Eq. (7) and from the produced  $H_2$  flow rate  $\dot{m}_{H_2}$  of Eq. (10), it is also possible to evaluate the relative equivalent  $CO_2$  emissions  $e_{CO_2, eq}$  [kg of  $CO_2, eq$ /kg of  $H_2$ ]:

$$e_{CO_2, eq} = \dot{m}_{CO_2, eq} / \dot{m}_{H_2} \quad (8)$$

It is also possible to define the equivalent NG thermal input  $\dot{Q}_{NG, eq}$  [MW] (for the cases with  $CO_2$  capture  $\dot{Q}_{NG, eq}^{capt}$  [MW] and for that without  $CO_2$  capture  $\dot{Q}_{NG, eq}^{no\ capt}$  [MW]):

$$\dot{Q}_{NG, eq} = \dot{m}_{NG}LHV_{NG} - \frac{Q_{th}}{\epsilon_{th}} - \frac{W_{el}}{\epsilon_{el}} \quad (9)$$

Indirect  $CO_2$  emissions and equivalent NG consumptions are taken into account in the definition of  $\eta_{H_2, eq}$  and SPECCA:

$$\eta_{H_2, eq} = \frac{\dot{m}_{H_2}LHV_{H_2}}{\dot{Q}_{NG, eq}} \quad (10)$$

$$SPECCA = \frac{\Delta(\eta_{H_2, eq})^{-1}}{\Delta e_{CO_2, eq}} = \frac{(\eta_{H_2, eq}^{capt})^{-1} - (\eta_{H_2, eq}^{no\ capt})^{-1}}{e_{CO_2, eq}^{no\ capt} - e_{CO_2, eq}^{capt}} \quad (11)$$

The equivalent-related parameters in Eqs. 10 and 11 take into account the energetic contributions of the co-production of thermal power  $Q_{th}$  [MW<sub>th</sub>] and/or electricity  $W_{el}$  [MW<sub>el</sub>] through the conversion efficiencies defined for Scenario 1 and Scenario 2 (Table 3). The SPECCA index gives an estimate of the additional amount of energy that is required to avoid the emissions to the atmosphere of a unit of  $CO_2$ , with respect to

the benchmark SMR case without capture. SPECCA values are comparable among the analysed case studies since they entail the same overall  $H_2$  output, otherwise both NG consumptions and equivalent  $CO_2$  emissions would need to be scaled over the  $H_2$  production.

Because of the different electricity balance and steam export among the assessed plants, a consistent comparison must take into account the indirect fuel consumption and indirect  $CO_2$  emissions associated to the electricity and steam flows. Ultimately, this allows the calculation of equivalent KPIs (Table 3):

- Scenario 1: Baseline Scenario. The reference thermal power is assumed to be produced through a NG boiler with efficiency of 90%, combustion emission factor of 2.75 kg  $CO_2$ /kg NG and resulting carbon intensity of 0.066 kg  $CO_2$ /MJ<sub>th</sub>. The reference electric power is assumed to be generated by a NG combined cycle (NGCC) without  $CO_2$  capture, with efficiency of 60% and carbon intensity of 345.0 kg  $CO_2$ /MWh<sub>el</sub>.
- Scenario 2: Low-Carbon Scenario. The reference thermal power is assumed to be produced through a NG boiler with efficiency of 90% and equipped with  $CO_2$  capture system able to separate 90% of the  $CO_2$ , which determines a combustion emission factor of 0.28 kg  $CO_2$ /kg NG (i.e., 0.008 kg  $CO_2$ /MJ<sub>th</sub>). The reference electric power is generated with a NGCC with  $CO_2$  capture hence, with an overall efficiency of 51% and carbon intensity equal to 35.0 kg  $CO_2$ /MWh<sub>el</sub> (i.e., 0.010 kg  $CO_2$ /MJ<sub>el</sub>).

## Results

This section describes the thermodynamic and economic results of the aforementioned plants. Additional results are reported in the Supplementary Material, as described in the text hereafter.

### Thermodynamic results

Thermodynamic results consist of mass and energy (chemical energy, electricity, steam) balances,  $CO_2$  balance, and overall  $CO_2$  avoidance (Tables 4 and 5).

The electric power output from the benchmark SMR case is equal to 10.4 MW<sub>el</sub>, which decreases in the case of MEA capture down to a negative value of −12.8 MW<sub>el</sub> (i.e., 12.8 MW<sub>el</sub> are imported from the grid, corresponding to 1.42 kWh<sub>el</sub>/kg of  $H_2$  produced), mainly due to the consumption for  $CO_2$  compression (7.2 MW<sub>el</sub>) and for the heat pump operation (2.8 MW<sub>el</sub>).

**Table 3 – Assumptions on the reference scenarios for the calculations of equivalent emissions: baseline scenario (Scenario 1) and decarbonised scenario (Scenario 2). Values are computed from a NG carbon intensity of 59.1 kg of  $CO_2$ /kg of NG (equivalent to the combustion of NG), and by assuming a carbon capture efficiency of 90% in Scenario 2.**

		Scenario 1	Scenario 2
NGCC plant efficiency	%	60%	51%
NGCC electricity carbon intensity	kg $CO_2$ /MWh	348	35
NG boiler efficiency	%	90%	70.3%

**Table 4 – Technical performance of the analysed plants in terms of: MCFC design, MCFC mass balances, and plant mass and energy balances.**

	Unit	SMR	SMR MEA	NGF	OGF	OGF-2	OGF-2-Deg
MCFC design							
Cell 1 potential	V	–	–	0.7	0.7	0.65	0.63
Cell 2 potential	V	–	–	–	–	0.60	0.59
UF	%	–	–	75.0%	75.0%	70.0%	68.1%
Cell 1 current density	A/m <sup>2</sup>	–	–	1565	1190	1674	1637
Cell 2 current density	A/m <sup>2</sup>	–	–	–	–	1008	991
Cell 1 area	m <sup>2</sup>	–	–	73123	41615	23605	23605
Cell 2 area	m <sup>2</sup>	–	–	–	–	9949	9949
Total cell area	m <sup>2</sup>	–	–	73123	41615	33554	33554
CO <sub>2</sub> utilisation factor	%	–	–	81.7%	77.5%	87.1%	85.1%
MCFC balances							
CO <sub>2</sub> conc. FTR comb. out	%	–	–	22.0%	11.8%	11.0%	11.0%
CO <sub>2</sub> conc. cathode in	%	–	–	4.7%	4.2%	6.3%	6.3%
Dry CO <sub>2</sub> conc. anode out	%	–	–	74.8%	84.8%	81.8%	80.7%
Dry CO <sub>2</sub> conc. CPU in	%	–	–	76.2%	85.5%	82.7%	81.7%
CO <sub>2</sub> prod. density cell 1	(g/s)/m <sup>2</sup>	–	–	0.360	0.556	0.646	0.643
CO <sub>2</sub> prod. density cell 2	(g/s)/m <sup>2</sup>	–	–	–	–	0.724	0.720
CO <sub>2</sub> flux through cell 1	(g/s)/m <sup>2</sup>	–	–	0.268	0.204	0.288	0.280
CO <sub>2</sub> flux through cell 2	(g/s)/m <sup>2</sup>	–	–	–	–	0.171	0.171
CO <sub>2</sub> permeation cell 1	kg/s	–	–	19.6	8.5	6.8	6.6
CO <sub>2</sub> permeation cell 2	kg/s	–	–	–	–	1.7	1.7
CO <sub>2</sub> permeation/storage	%	–	–	78.6%	37.2%	35.7%	35.2%
Mass and energy balances							
Total NG in	kg/s	8.76	8.76	11.02	9.51	9.45	9.45
Total NG thermal in	MW <sub>LHV</sub>	407.3	407.3	512.4	442.2	439.4	439.4
NG in to SMR	%	100.0%	100.0%	68.6%	100.0%	100.0%	100.0%
of which to FTR comb.	%	17.4%	17.4%	17.2%	28.2%	28.8%	28.8%
of which to SMR reform.	%	82.6%	82.6%	82.8%	71.8%	71.2%	71.2%
NG in to MCFC anode	%	0.0%	0.0%	31.4%	0.0%	0.0%	0.0%
PSA off-gas	MW <sub>LHV</sub>	97.1	97.1	90.8	95.0	94.6	94.8
of which to FTR comb.	%	100.0%	100.0%	100.0%	18.9%	12.2%	12.2%
of which to MCFC anode	%	0.0%	0.0%	0.0%	81.8%	87.8%	87.8%

The steam thermal output from the benchmark SMR is equal to 23.2 MW<sub>th</sub>, which reduces to 0 MW<sub>th</sub> in the SMR with MEA case. The MCFC plants require additional NG input (between +8% and +26% depending on the cases). This additional fuel input leads to higher net electricity export (22.1–59.1 MW<sub>el</sub> vs. 10.4 MW<sub>el</sub>) and similar steam export (21.5–24.6 MW<sub>th</sub> vs. 23.2 MW<sub>th</sub>) compared to the reference plant without capture. As for the performance in terms of CO<sub>2</sub> capture, the SMR with MEA case has similar results to the OGF system in terms of CCR (90.0% vs. 90.3%), with the NGF option entailing a slightly worse CO<sub>2</sub> separation (85.0%). On the other hand, both NGF and (particularly) OGF exhibit better results in terms of equivalent emissions, with a relative equivalent CO<sub>2</sub> emission close to 0 kg CO<sub>2,eq</sub>/kg H<sub>2</sub> or even negative, depending on the chosen reference scenario for indirect emissions (thanks to the heat and power export leading to lower equivalent CO<sub>2</sub> avoided than the benchmark plant without CO<sub>2</sub> capture, which leads to a decarbonised electric grid as a co-benefit). The H<sub>2</sub> production efficiency is higher in the SMR with MEA case (73.5%) with respect to the NGF plant (58.5%) and the OGF one (67.7%). This is due to the additional NG input of the MCFC-based plants, which is needed either in the fuel cell (NGF case) or to compensate the loss of PSA off-gas fuel in the SMR burners (OGF case). Oppositely, NGF and OGF exhibit a much higher H<sub>2</sub> equivalent production efficiency (up to 80.4% for NGF and 80.6% for OGF) with respect to the SMR with MEA

plant (69.2%). The good equivalent efficiency and emissions lead to low values of SPECCA (between 0.6 and 1.1 MJ/kg CO<sub>2</sub> for NGF and between 0.5 and 0.6 MJ/kg CO<sub>2</sub> for OGF) compared to the SMR with MEA (between 3.7 and 3.8 MJ/kg CO<sub>2</sub>).

NGF case exhibits a higher CO<sub>2</sub> utilisation factor (81.7%) with respect to OGF (77.5%), which results from the higher cooling of the cell deriving from the endothermic steam methane reforming when NG is used as MCFC fuel. This involves a lower demand of air to cool down the MCFC and lower dilution of the SMR flue gas with air at the cathode inlet. NGF has larger CO<sub>2</sub> permeation from the cathode to the anode, which results in a larger exploitation of the separation capabilities of the cell itself. This is testified by the relative CO<sub>2</sub> permeation over storage<sup>1</sup> which is equal to 78.6% (NGF) against a lower 37.2% for OGF (Fig. 6). This results in a 43% smaller area in OGF with respect to NGF, as shown by the lower CO<sub>2</sub> flow rate separated by the MCFC (8.5 vs. 19.6 kg/s). The CO<sub>2</sub> flux through the cell<sup>2</sup> is lower in OGF (0.204 vs. 0.268 g/s/m<sup>2</sup>), but CO<sub>2</sub> production density<sup>3</sup> is 54% higher, as only 37.2%

<sup>1</sup> The relative CO<sub>2</sub> permeation over storage is the flow rate of CO<sub>2</sub> separated in the MCFC with respect to the compressed CO<sub>2</sub> delivered by the plant to the CO<sub>2</sub> transport infrastructure.

<sup>2</sup> The specific flux throughout the cell is the ratio between the mass flow rate of permeating CO<sub>2</sub> and the area of the cell.

<sup>3</sup> The CO<sub>2</sub> production density is the ratio between the total CO<sub>2</sub> mass flow rate at the cathode outlet and the area of the cell.

**Table 5 – Technical performance of the analysed plants in terms of: plant electricity and steam balance, CO<sub>2</sub> balance and plant performance, and equivalent performance indicators.**

	Unit	SMR	SMR MEA	NGF	OGF	OGF-2	OGF-2-Deg
MCFC design							
Cell 1 potential	V	–	–	0.7	0.7	0.65	0.63
Cell 2 potential	V	–	–	–	–	0.60	0.59
UF	%	–	–	75.0%	75.0%	70.0%	68.1%
Electricity and steam balance							
LP + HP turb. power out	MW <sub>el</sub>	12.2	0.0	10.5	11.1	9.2	9.2
Cell 1 net power out	MW <sub>el</sub>	–	–	74.2	32.1	23.8	22.4
Cell 1 power density	W/m <sup>2</sup>	–	–	1014.7	771.3	1008.3	950.6
Cell 2 net power out	MW <sub>el</sub>	–	–	–	–	5.6	5.4
Cell 2 power density	W/m <sup>2</sup>	–	–	–	–	562.9	540.8
Auxiliaries	MW <sub>el</sub>	–1.2	–4.0	–9.1	–5.0	–2.4	–2.5
CPU/others	MW <sub>el</sub>	0.0	–7.5	–15.2	–11.7	–13.1	–13.2
Net electric power out	MW <sub>el</sub>	10.4	–12.8	59.1	22.1	19.8	18.1
LP steam export	kg/s	10.9	0.0	9.9	11.3	12.1	12.0
Steam thermal out	MW <sub>th</sub>	23.2	0.0	21.5	24.6	26.2	26.0
CO <sub>2</sub> balance and plant performance							
CO <sub>2</sub> emitted	kgCO <sub>2</sub> /s	23.2	2.3	4.4	2.5	1.3	1.5
CO <sub>2</sub> captured	kgCO <sub>2</sub> /s	0.0	20.9	24.9	22.8	23.8	23.6
Specific CO <sub>2</sub> emission	kgCO <sub>2</sub> /kgH <sub>2</sub>	9.29	0.93	1.75	0.98	0.50	0.58
H <sub>2</sub> production efficiency	%	73.5%	73.5%	58.5%	67.7%	68.2%	68.5%
CCR	%	0.0%	90%	85.0%	90.3%	95.0%	94.2%
Equivalent performance indicators							
Eq. CO <sub>2</sub> em. (Scen.1)	kgCO <sub>2,eq</sub> /kgH <sub>2</sub>	8.3	1.4	–1.1	–0.5	–1.0	–0.8
Eq. CO <sub>2</sub> em. (Scen.2)	kgCO <sub>2,eq</sub> /kgH <sub>2</sub>	9.2	1.0	1.5	0.8	0.3	0.4
Eq. H <sub>2</sub> prod. eff. (Scen.1)	%	82.3%	69.9%	76.8%	79.2%	79.4%	79.1%
Eq. H <sub>2</sub> prod. eff. (Scen.2)	%	83.0%	69.2%	80.4%	80.6%	80.6%	80.2%
SPECCA (Scen.1)	MJ/kgCO <sub>2</sub>	0.0	3.8	1.1	0.6	0.6	0.7
SPECCA (Scen.2)	MJ/kgCO <sub>2</sub>	0.0	3.5	0.6	0.5	0.5	0.6

of the captured CO<sub>2</sub> flows through the cell, vs. 78.6% in the NGF case. The lower CO<sub>2</sub> permeation in OGF determines a lower NG consumption with respect to NGF. In the NGF case the NG is uniquely used as fuel and feed in the SMR, while in OGF most of the PSA off-gas (81.8%) is fed to the MCFC and the remaining part to the SMR burners. In short, due to the higher capture rate, the higher H<sub>2</sub> production efficiency, the lower SPECCA and the significantly lower MCFC area, the OGF case is superior to the NGF one. We therefore consider OGF as process layout for the analyses presented below (sensitivity analyses on variations of the cell potential and UF are reported in the Supplementary Material).

OGF-2 (i.e., two MCFCs in series with inter-cooling) represents a highly beneficial design to maximise the capabilities of the cells in separating CO<sub>2</sub>. Not surprisingly, this configuration is characterised by a higher electric power output (due to the combined effects of higher electricity output from the cells and lower utilities consumptions for air inlet to the cathode) and by a lower cell area with respect to OGF. Moreover, the CCR increases over 95%, with stable H<sub>2</sub> production efficiency and higher CO<sub>2</sub> utilisation factor (higher than 87%). As for the areas of the cells, the OGF-2 plant is characterised by a first cell (23605 m<sup>2</sup> for 0.65 V) which is larger than the second one (9949 m<sup>2</sup> for 0.60 V). The first cell is also characterised by a higher electric power density (1008.3 W/m<sup>2</sup>) with respect to cell 2 (562.9 W/m<sup>2</sup>).

Notoriously, in fuel cells application the cell degradation has often been regarded as a key factor hindering economics and deployment. Therefore, we decided to investigate the change in performance when degradation takes place. As

expected, the effect of cell degradation is a decrease in the performance of the cells (defined as a gradual degradation phase, followed by a rapid degradation phase, as shown in Morita et al. [53]). When compared to case OGF-2, OGF-2-Deg exhibits lower CO<sub>2</sub> utilisation factor (from 87.1% to 85.1%) and lower UF (from 70.0% to 68.1%), in turn producing a marginally larger output of H<sub>2</sub>. The power output from the cells decreases by 6% (cell 1) and 4% (cell 2), with a net electric power output of 18.1 MW<sub>el</sub> (against 19.8 MW<sub>el</sub> in OGF-2). The steam export is almost unchanged. The global result in terms of CO<sub>2</sub> capture is a limited decrease in the CCR (from 95.0% to 94.2%). As the effect of degradation is a shift in the polarisation curves of both cells towards lower potential, the new operating points lay on the degraded polarisation curve with marginal differences in the resulting current density with respect to the OGF-2 original cases (0.63 and 0.59 V vs. 0.65 and 0.60 V, with about 2% decrease in current density). The new degraded operating points would represent the operational parameters (potential and current density) of cells when degradation phenomena have fully occurred. At this point, based on the public knowledge from lab tests, the cells may need to be replaced to avoid entering in the region of rapid non-linear degradation.

## Economic results

### Baseline results

While the thermodynamic results have confirmed the potential of MCFCs integration in SMR, their deployment would be eventually driven by their costs compared to other low-CO<sub>2</sub>

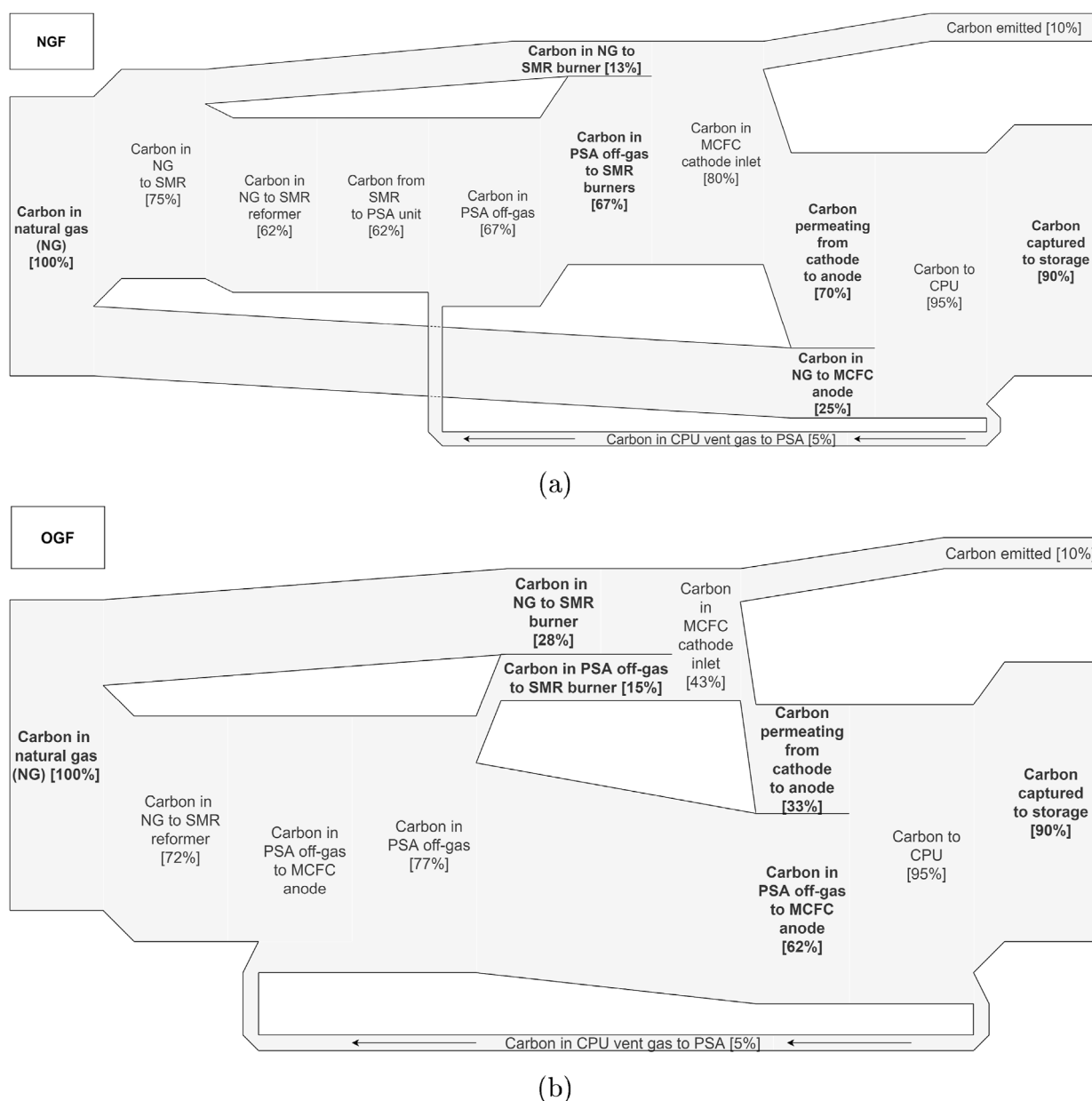


Fig. 6 – Sankey diagrammes of carbon streams for (a) NGF and (b) OGF.

solutions. The results of the economic analysis in terms of TDPC are reported in Fig. 7a. It emerges that the SMR with MEA has a lower capital expenditure (197.3 M€) compared to the MCFC-based alternatives, considering that the NGF case costs 245.5 M€ (i.e., +24.4% with respect to SMR with MEA), while the OGF case has a cost of 206.9 M€ (+4.9%, which is nonetheless a limited increase considering its better environmental performance). A decrease in capital costs can be achieved through the OGF-2 configuration. In fact, OGF-2 entails a TDPC of 190.3 M€ (i.e., competitive with the SMR with MEA plant), thanks to limited expenditures in the MCFC stack (i.e., 30.9 M€) coupled with savings in heat exchangers (in particular, the air pre-heaters). The effect of including the cell replacement cost every 5 years within the capital expenditure can be observed in the annualised TDPC (Fig. 7b). As costs increase in all MCFC-based scenarios proportionally to the

area of the cell, those plants characterised by a small cell area manage to keep a limited spread of cost with respect to the reference SMR plant with MEA. In particular, NGF costs 30.0 M€/year (i.e., +75.3% with respect to SMR with MEA), OFG costs 22.9 M€/year (i.e., +33.8%), while OGF-2 costs 21.0 M€/year (i.e., +22.6%). Overall, the total MCFC stack cost (including both the original investment and the cyclic replacement of the cell) accounts for up to half of the total capital expenditure, being the NGF case the most expensive (46.4% of 30.0 M€/year total).

The yearly total cost and revenues and the resulting H<sub>2</sub> production cost are reported in Fig. 8. The largest share of the yearly total costs is constituted by the NG cost, which accounts for 47.3–52.6% (NGF), 49.2–52.5% (OGF), and 51.8–55.4% (OGF-2) of the net total, depending on the scenario. Importantly, MCFC-based plants always produce



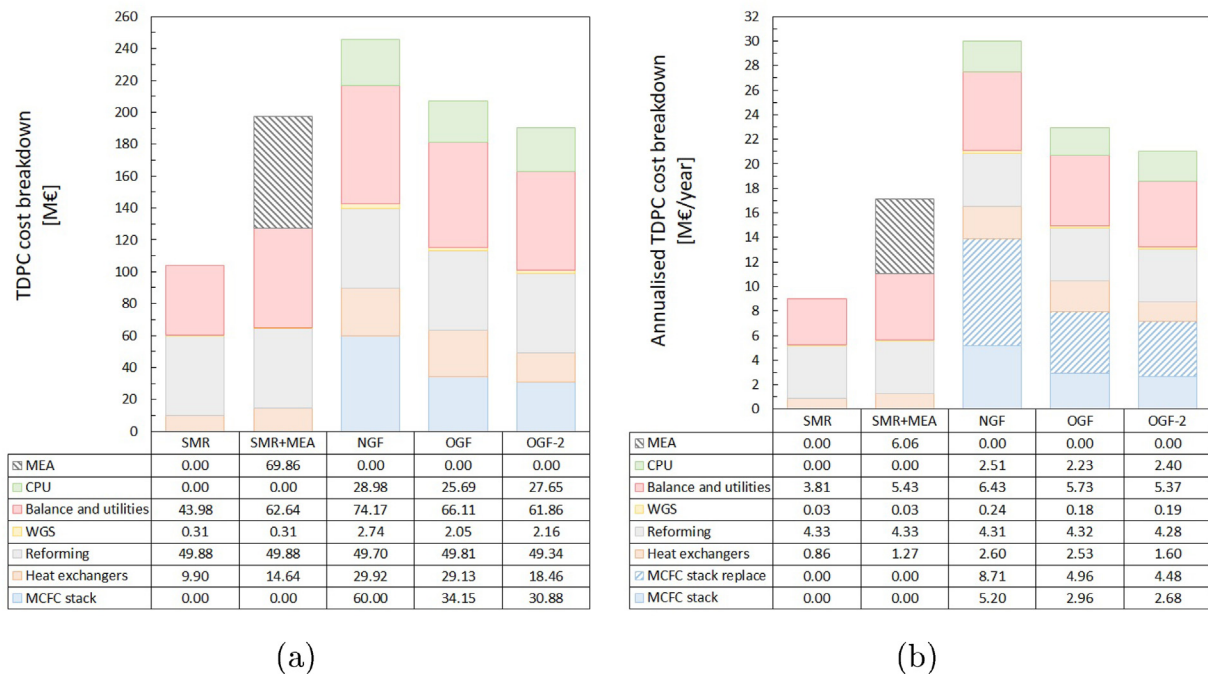


Fig. 7 – Material and installation costs: (a) total direct plant cost TDPC [M€], and (b) annualised TDPC [M€/year].

quotas of electricity and steam that are available for export and that generate additional revenues compared to the reference SMR with MEA. Overall, OGF and OGF-2 plants exhibit a  $H_2$  production cost that is comparable or lower

(between 1.9 and 2.0 €/kg of  $H_2$  and 2.0–2.2 €/kg of  $H_2$ ) than that obtained in the reference SMR with MEA (2.2–2.3 €/kg of  $H_2$ ). Cell degradation has a very small impact on the  $H_2$  production cost (+0.2%).

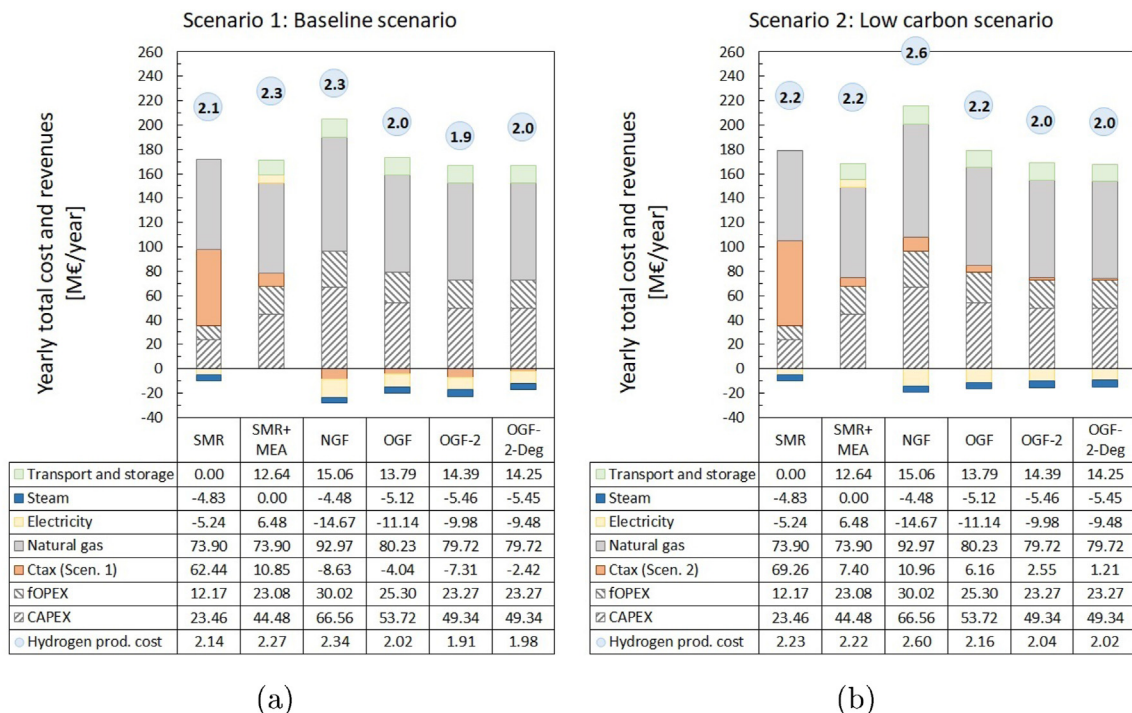
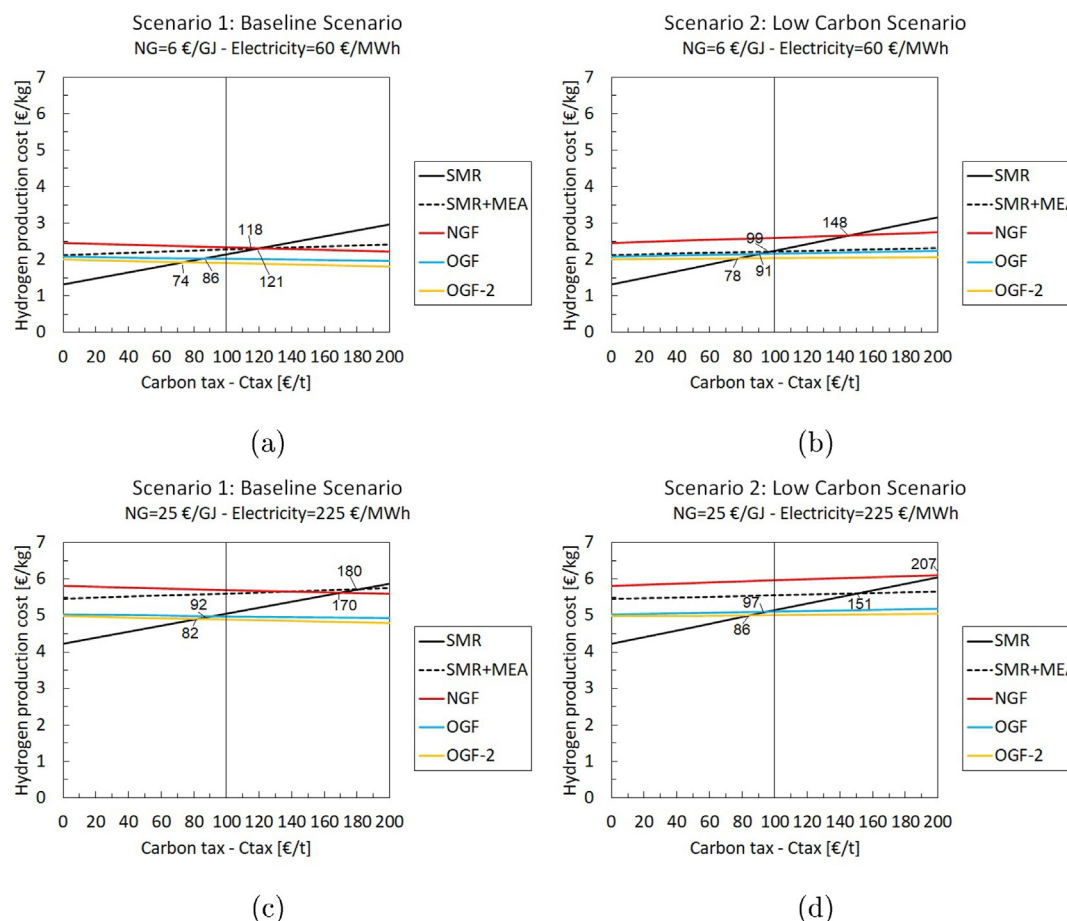


Fig. 8 – Total costs and  $H_2$  production cost: (a) Scenario 1: Baseline scenario, and (b) Scenario 2: Low carbon scenario. The specific  $H_2$  production cost [€/kg of  $H_2$ ] is shown in the circles above the bars.





**Fig. 9 – Sensitivity analysis on carbon tax (Ctax) over H<sub>2</sub> production cost for different combinations of NG and electricity unitary costs: (a,c) Scenario 1: Baseline scenario, and (b,d) Scenario 2: Low carbon scenario.**

#### Sensitivity analyses: carbon tax and unitary costs

Indeed, several uncertainties exist in this economic analysis. We therefore carried out sensitivity analyses to check the robustness of the results; results are reported in the following and in the Supplementary Material. Firstly, the introduction of a carbon tax [€/t] applied on equivalent emissions may significantly affect the economic results in terms of H<sub>2</sub> production cost. In particular, Fig. 9 describes the variation of H<sub>2</sub> production cost as an outcome of setting a carbon tax in the range of 0–200 €/t (where cases with negative slopes reflect those with lower equivalent CO<sub>2</sub> emissions than the benchmark plant without capture). This analysis is performed for two options of NG cost and electricity price: an optimistic case with NG at 6 €/GJ and electricity at 60 €/MWh (i.e., baseline values), and a case with NG at 25 €/GJ and electricity at 225 €/MWh. The intersections between the cost curve of H<sub>2</sub> production without capture (i.e., SMR) and those resulting from either a MEA-based (i.e., SMR with MEA) or MCFC-based (i.e., NGF, OGF, and OGF-2) plants give the break-even value of carbon tax (hence, the cost of CO<sub>2</sub> avoided) that would make economically attractive the use of an integrated SMR with CO<sub>2</sub> capture, with respect to the unabated SMR. In particular, for a low cost of NG and low price of electricity, H<sub>2</sub> production with OGF-2 becomes cost competitive with the unabated SMR for a

carbon tax of 74.3 €/t (Scenario 1) or 77.7 €/t (Scenario 2), the OGF plant for a carbon tax of 86.2 €/t (Scenario 1) or 90.9 €/t (Scenario 2), while the NGF plant for a carbon tax of 121.0 €/t (Scenario 1) or 147.5 €/t (Scenario 2). When compared with the reference system with MEA capture, the OGF and OGF-2 plants are cost competitive for the entire range of investigated carbon tax. If the NG cost and electricity price are increased to 25 €/GJ and 225 €/MWh, respectively, MCFC-based CO<sub>2</sub> capture entails lower H<sub>2</sub> production costs with respect to the reference MEA plant over the entire range of carbon tax investigated here, with the only exception being the NGF plant.

The economic results were evaluated on variations of: NG cost (up to 30 €/GJ), electricity price (up to 300 €/MWh), and simultaneous variations of NG cost (up to 30 €/GJ) and electricity price (assumed equal to 2.5 times the price of NG for industrial use) (Fig. 10). All the analysed case studies exhibit a noticeable variation in H<sub>2</sub> production cost depending on the unitary cost of NG. MCFC-based systems entail a H<sub>2</sub> production cost varying between a minimum of 0.9–1.0 €/kg of H<sub>2</sub> (for NG at 0 €/GJ) up to a maximum of 7.3–7.5 €/kg of H<sub>2</sub> (for NG at 30 €/GJ), being the NGF case always the most expensive plant design, whereas OGF and OGF-2 have similar production costs and are generally comparable with the reference SMR with MEA. Contrary to the SMR with MEA, an increase in

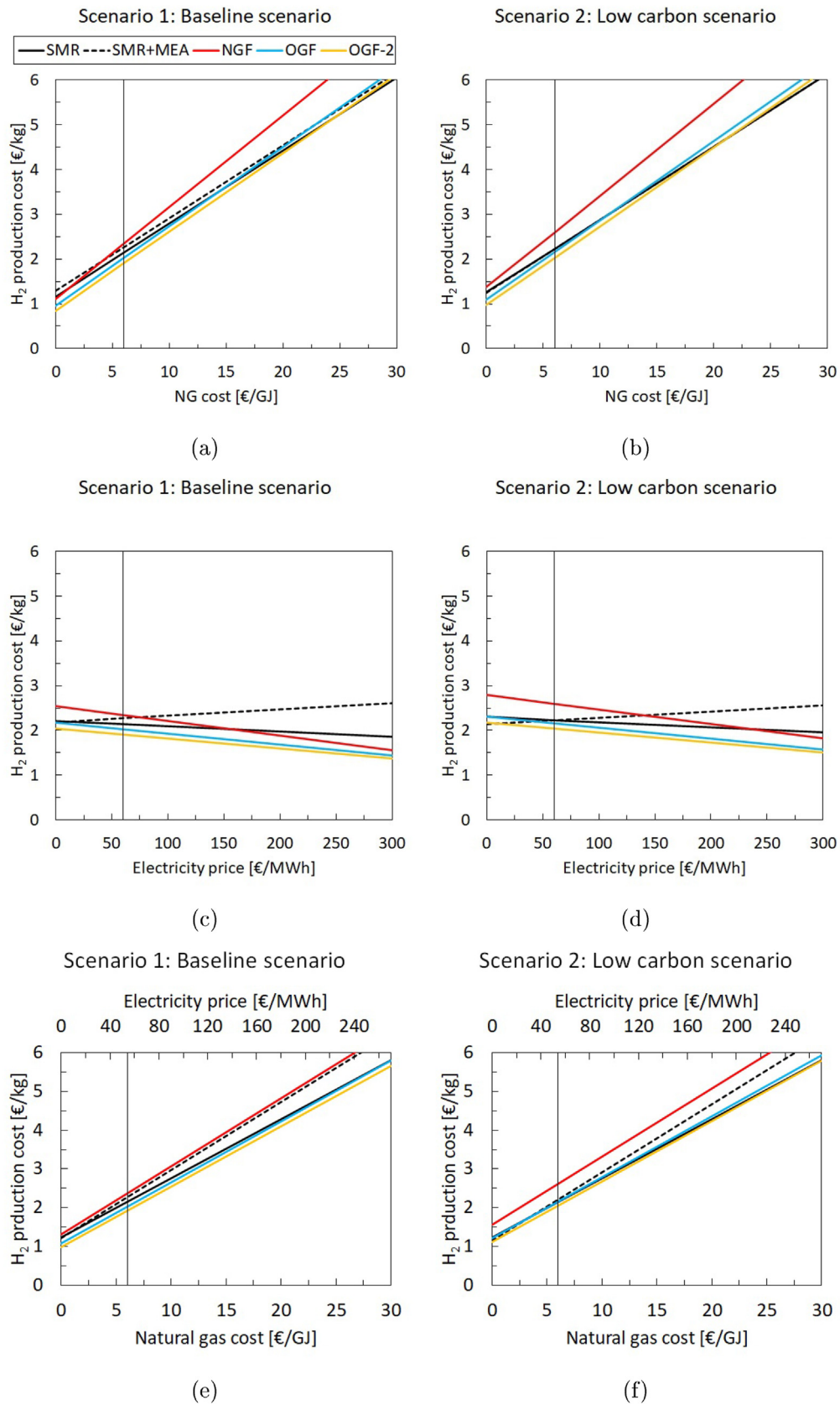
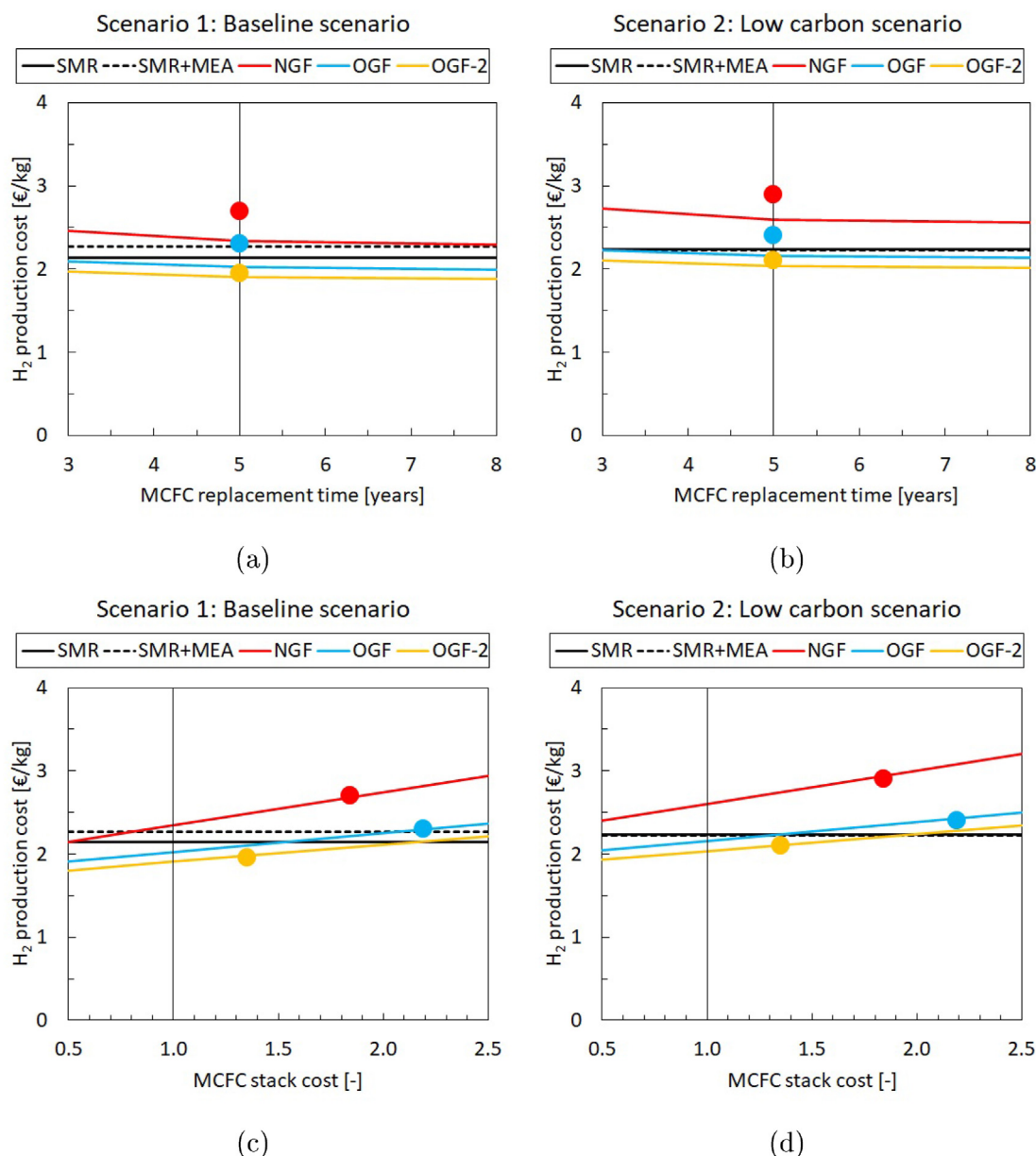


Fig. 10 – Sensitivity analyses on: (a,b) NG cost, (c,d) electricity price, and (e,f) correlated variation of NG cost and electricity price.



**Fig. 11 – Sensitivity analyses on: (a,b) MCFC replacement time, and (c,d) MCFC stack cost relative variation over baseline value. The circles represent the costs resulting from the use of an alternative MCFC model, which is reported in the Supplementary Material.**

electricity price causes a decrease in H<sub>2</sub> production cost in all MCFC-based plants, being these net electricity exporters. When considering correlated variations of NG cost and electricity price, MCFC-based plants become cost-competitive with the reference SMR with MEA in terms of H<sub>2</sub> production cost, with the exception of NGF.

The sensitivities of the economic outcomes on the MCFC stack cost (up to 2.5 times the baseline investment cost) and replacement time (from 3 years to 8 years) are reported in Fig. 11. In particular, the sensitivity analysis on the MCFC stack cost reflects the uncertainty in its assumed specific investment cost and sizing, as testified by the different techno-economic results that would be obtained by choosing an alternative MCFC model (see Supplementary

Material). As for the H<sub>2</sub> production cost, the NGF plant is always more expensive than its OGF alternative and, most importantly, than the reference SMR with MEA (2.2–2.3 €/kg) for the entire investigated range of MCFC cost and replacement time. On the other hand, OGF and OGF-2 show lower production costs than the SMR with MEA when the MCFC stack is at maximum as expensive as 1.5–2 times its assumed nominal value.

## Conclusions

This study provides a techno-economic assessment of integrated steam methane reforming with molten carbonate fuel

cell CO<sub>2</sub> capture to produce blue H<sub>2</sub>. Different plant designs were investigated depending on the fuel anode inlet, namely a conventional natural gas feed (i.e., NGF), a novel process based on off-gas feed deriving from the H<sub>2</sub> purification unit of steam methane reforming (i.e., OGF), and a 2-stage cell with inter-cooling based on off-gas feed (i.e., OFG-2). The performance of these plants was compared with steam methane reforming with conventional CO<sub>2</sub> post-combustion capture via monoethanolamine solvent. The following emerged:

- Molten carbonate fuel cell plants consume more natural gas with respect to the standalone steam methane reforming (between +8% and +26%), but they also generate a larger low-carbon electricity output.
- OGF appears superior compared to NGF, being the former characterised by higher carbon capture rate (90% against 85%), higher H<sub>2</sub> production efficiency (68% against 59%), lower specific energy consumption per unit of CO<sub>2</sub> avoided (0.5 against 1.1 MJ/kg of CO<sub>2</sub>), and a significantly lower cell area (−43%). This outcome is due to the higher carbon intensity of the off-gas feed to the OGF cell anode, compared to the natural gas exploited in the NGF case, which allows reducing the flow rate of CO<sub>2</sub> to be separated by the molten carbonate fuel cell for a given CO<sub>2</sub> capture rate.
- OGF-2 is a particularly competitive configuration, as it can achieve 95% carbon capture rate with a smaller cell area than OGF (−19%). This is due to the inter-cooling between cells, which allows reducing the CO<sub>2</sub> dilution resulting from the excess air to be mixed with the flue gas to control the MCFC temperature.
- OGF and OGF-2 plants exhibit H<sub>2</sub> production costs (1.9–2.2 €/kg of H<sub>2</sub>) that are lower than NGF (2.3–2.6 €/kg of H<sub>2</sub>) and than steam methane reforming with conventional post-combustion CO<sub>2</sub> capture (2.2–2.3 €/kg of H<sub>2</sub>). The sensitivity analyses on key economic parameters (e.g., carbon tax, natural gas cost, electricity price) did not affect significantly the main outcome, i.e., the good economic performance of OGF and OGF-2. Contrary to the NGF case, the OGF one (and especially the 2-stage configuration) emerged as cost competitive with conventional solvent-based post-combustion capture in the entire range of values explored in the sensitivities.
- Cell degradation inducing a 5% reduction in the MCFC voltage (i.e., gradual degradation expected before the rapid performance decay) has limited impact on the heat and mass balances of the plant, thus on the overall economic performance. At the same time, an analysis on the stack replacement time showed that replacing the cell every 5 years appears as a good target, considering the minor improvement in costs for larger time horizons (from 5 to 8 years) and the considerable worsening of the economic performance when a reduced replacement time is considered (from 5 to 3 years).

Overall, the results obtained in this conceptual study highlight the potential of molten carbonate fuel cells as post-combustion CO<sub>2</sub> capture systems in blue hydrogen plants, if fed with pressure swing adsorption (PSA) off-gas as fuel. Molten carbonate fuel cell-based OGF and OGF-2 cases

showed a better performance compared to monoethanolamine solvent-based capture system in a wide range of natural gas and electricity prices. The highest uncertainty of the study is related to the molten carbonate fuel cell surface area required to achieve a target CO<sub>2</sub> capture rate and its performance over prolonged testing time, which requires experimental validation at scale. Public transparent data in the literature on molten carbonate fuel cells behaviour are scarce and predictions based of alternative models may lead to significantly different sizes, with important effects on the economic performance indicators.

## Authors contributions

Conceptualisation: LMP, MCR; Formal analysis: FdA; Funding acquisition: MG, MCR; Investigation: FdA; Methodology: FdA, MG, MCR, SC; Supervision: MG, MCR; Writing - original draft: FdA; Writing - review and editing: FdA, LMP, SC, MG, MCR.

## Declaration of competing interest

The authors declare that they have no known competing financial interests or personal relationships that could have appeared to influence the work reported in this paper.

## Acknowledgements

This work has been funded by TotalEnergies' R&D Strategic Anticipation Program.

## Appendix A. Supplementary data

Supplementary data to this article can be found online at <https://doi.org/10.1016/j.ijhydene.2023.06.137>.

## REFERENCES

- [1] van der Spek M, Banet C, Bauer C, Gabrielli P, Goldthorpe W, Mazzotti M, Munkejord ST, Røkke NA, Shah N, Sunny N, Sutter D, Trusler JM, Gazzani M. Perspective on the hydrogen economy as a pathway to reach net-zero CO<sub>2</sub> emissions in Europe. *Energy Environ Sci* 2022;15:1034–77. <https://doi.org/10.1039/d1ee02118d>.
- [2] Bauer C, Treyer K, Antonini C, Bergerson J, Gazzani M, Gencer E, Gibbins J, Mazzotti M, McCoy ST, McKenna R, Pietzcker R, Ravikumar AP, Romano MC, Ueckerdt F, Vente J, van der Spek M. On the climate impacts of blue hydrogen production. *Sustain Energy Fuels* 2022;6:66–75. <https://doi.org/10.1039/d1se01508g>.
- [3] Pettersen J, Steeneveldt R, Grainger D, Scott T, Holst LM, Hamborg ES. Blue hydrogen must be done properly. *Energy Sci Eng* 2022;10:3220–36. <https://doi.org/10.1002/ese3.1232>.
- [4] IEAGHG. Understanding the cost of retrofitting CO<sub>2</sub> capture in an integrated oil refinery. 2017. <https://ieaghg.org/publications/technical-reports/reports-list/10-technical->



- reviews/819-2017-tr8-understanding-the-cost-of-retrofitting-co2-capture-in-an-integrated-oil-refinery. [Accessed 3 February 2023].
- [5] FuelsEurope. Statistical report. 2020. [https://www.fuels-europe.eu/wp-content/uploads/SR\\_FuelsEurope\\_2020-1.pdf](https://www.fuels-europe.eu/wp-content/uploads/SR_FuelsEurope_2020-1.pdf). [Accessed 3 February 2023].
  - [6] IEA. Global energy-related CO<sub>2</sub> emissions by sector. 2022. <https://www.iea.org/data-and-statistics/charts/global-energy-related-co2-emissions-by-sector>. [Accessed 3 February 2023].
  - [7] IEAGHG. Techno-economic evaluation of SMR based standalone (merchant) hydrogen plant with CCS. 2017. [https://ieaghg.org/exco\\_docs/2017-02.pdf](https://ieaghg.org/exco_docs/2017-02.pdf). [Accessed 3 February 2023].
  - [8] Oni AO, Anaya K, Giwa T, Di Lullo G, Kumar A. Comparative assessment of blue hydrogen from steam methane reforming, autothermal reforming, and natural gas decomposition technologies for natural gas-producing regions. *Energy Convers Manag* 2022;254:115245. <https://doi.org/10.1016/j.enconman.2022.115245>.
  - [9] Wismann ST, Engbaek JS, Vendelbo SB, Bendixen FB, Eriksen WL, Aasberg-Petersen K, Frandsen C, Chorkendorff IB, Mortensen PM. Electrified methane reforming: a compact approach to greener industrial hydrogen production. *Science* 2019;364:756–9. <https://doi.org/10.1126/science.aaw8775>.
  - [10] IEAGHG. Low-carbon hydrogen from natural gas: global roadmap. 2022. <https://ieaghg.org/ccs-resources/blog/new-ieaghg-technical-report-2022-07-low-carbon-hydrogen-from-natural-gas-global-roadmap>. [Accessed 24 March 2023].
  - [11] Milewski J, Cwieka K, Szczęśniak A, Ł Szabłowski, Wejrzanowski T, Skibinski J, Dybiński O, Lysik A, Sienko A, Stanger P. Recycling electronic scrap to make molten carbonate fuel cell cathodes. *Int J Hydrogen Energy* 2021;48:11831–43. <https://doi.org/10.1016/j.ijhydene.2021.11.247>.
  - [12] Chiesa P, Campanari S, Manzolini G. CO<sub>2</sub> cryogenic separation from combined cycles integrated with molten carbonate fuel cells. *Int J Hydrogen Energy* 2011;36:10355–65. <https://doi.org/10.1016/j.ijhydene.2010.09.068>.
  - [13] Spinelli M, Campanari S, Consonni S, Romano MC, Kreutz T, Ghezal-Ayagh H, Jolly S. Molten carbonate fuel cells for retrofitting post-combustion CO<sub>2</sub> capture in coal and natural gas power plants. *J Electrochem Energy Convers Storage* 2018;15:1–15. <https://doi.org/10.1115/1.4038601>.
  - [14] Rosen J, Geary T, Hilmi A, Blanco-Gutierrez R, Yuh CY, Pereira CS, Han L, Johnson RA, Willman CA, Ghezal-Ayagh H, Barckholtz TA. Molten carbonate fuel cell performance for CO<sub>2</sub> capture from natural gas combined cycle flue gas. *J Electrochem Soc* 2020;167:064505. <https://doi.org/10.1149/1945-7111/ab7a9f>.
  - [15] Spinelli M, Romano MC, Consonni S, Campanari S, Marchi M, Cinti G. Application of molten carbonate fuel cells in cement plants for CO<sub>2</sub> capture and clean power generation. *Energy Proc* 2014;63:6517–26. <https://doi.org/10.1016/j.egypro.2014.11.687>.
  - [16] Mastropasqua L, Pierangelo L, Spinelli M, Romano MC, Campanari S, Consonni S. Molten Carbonate Fuel Cells retrofits for CO<sub>2</sub> capture and enhanced energy production in the steel industry. *Int J Greenh Gas Control* 2019;88:195–208. <https://doi.org/10.1016/j.ijggc.2019.05.033>.
  - [17] Consonni S, Mastropasqua L, Spinelli M, Barckholtz TA, Campanari S. Low-carbon hydrogen via integration of steam methane reforming with molten carbonate fuel cells at low fuel utilization. *Adv Appl Energy* 2021;2:100010. <https://doi.org/10.1016/j.adapen.2021.100010>.
  - [18] Baccioli A, Liponi A, Milewski J, Szczęśniak A, Desideri U. Hybridization of an internal combustion engine with a molten carbonate fuel cell for marine applications. *Appl Energy* 2021;298:117192. <https://doi.org/10.1016/j.apenergy.2021.117192>.
  - [19] FuelCell Energy. Pilot test of novel electrochemical membrane system for carbon dioxide capture and power generation. 2018. <https://www.osti.gov/servlets/purl/1484012>. [Accessed 3 February 2023].
  - [20] FuelCell Energy. Pre-FEED study of a MW-class molten carbonate fuel cell system for carbon capture demonstration at an oil sands facility. 2017. <https://albertainnovates.ca/app/uploads/2020/10/FuelCell-Energy-Pre-FEED-Study-of-a-MW-Class-Molten-Carbonate-Fuel-Cell-System-for-Carbon-Capture-Demonstration-at-an-Oil-Sands-Facility.pdf>. [Accessed 3 February 2023].
  - [21] Barckholtz TA, Taylor KM, Narayanan S, Jolly S, Ghezal-Ayagh H. Molten carbonate fuel cells for simultaneous CO<sub>2</sub> capture, power generation, and H<sub>2</sub> generation. *Appl Energy* 2022;313:118553. <https://doi.org/10.1016/j.apenergy.2022.118553>.
  - [22] Campanari S. Carbon dioxide separation from high temperature fuel cell power plants. *J Power Sources* 2002;112:273–89. [https://doi.org/10.1016/S0378-7753\(02\)00395-6](https://doi.org/10.1016/S0378-7753(02)00395-6).
  - [23] Sugiura K, Takei K, Tanimoto K, Miyazaki Y. The carbon dioxide concentrator by using MCFC. *J Power Sources* 2003;118:218–27. [https://doi.org/10.1016/S0378-7753\(03\)00084-3](https://doi.org/10.1016/S0378-7753(03)00084-3).
  - [24] Milewski J, Lewandowski J. Separating CO<sub>2</sub> from flue gases using a molten carbonate fuel cell. *IERI Procedia* 2012;1:232–7. <https://doi.org/10.1016/j.ieri.2012.06.036>.
  - [25] Duan L, Xia K, Feng T, Jia S, Bian J. Study on coal-fired power plant with CO<sub>2</sub> capture by integrating molten carbonate fuel cell system. *Energy* 2016;117:578–89. <https://doi.org/10.1016/j.energy.2016.03.063>.
  - [26] Samanta S, Ghosh S. A thermo-economic analysis of repowering of a 250 MW coal fired power plant through integration of Molten Carbonate Fuel Cell with carbon capture. *Int J Greenh Gas Control* 2016;51:48–55. <https://doi.org/10.1016/j.ijggc.2016.04.021>.
  - [27] Samanta S, Ghosh S. Techno-economic assessment of a repowering scheme for a coal fired power plant through upstream integration of SOFC and downstream integration of MCFC. *Int J Greenh Gas Control* 2017;64:234–45. <https://doi.org/10.1016/j.ijggc.2017.07.020>.
  - [28] Carapellucci R, Di Battista D, Cipollone R. The retrofitting of a coal-fired subcritical steam power plant for carbon dioxide capture: a comparison between MCFC-based active systems and conventional MEA. *Energy Convers Manag* 2019;194:124–39. <https://doi.org/10.1016/j.enconman.2019.04.077>.
  - [29] Cooper R, Bove D, Audasso E, Ferrari MC, Bosio B. A feasibility assessment of a retrofit Molten Carbonate Fuel Cell coal-fired plant for flue gas CO<sub>2</sub> segregation. *Int J Hydrogen Energy* 2021;46:15024–31. <https://doi.org/10.1016/j.ijhydene.2020.09.189>.
  - [30] Lusardi M, Bosio B, Arato E. An example of innovative application in fuel cell system development: CO<sub>2</sub> segregation using Molten Carbonate Fuel Cells. *J Power Sources* 2004;131:351–60. <https://doi.org/10.1016/j.jpowsour.2003.11.091>.
  - [31] Chiappini D, Andreassi L, Jannelli E, Ubertini S. Ultralow carbon dioxide emission MCFC based power plant. *J Fuel Cell Sci Technol* 2011;8:2–9. <https://doi.org/10.1115/1.4002903>.
  - [32] Milewski J, Bernat R, Lewandowski J. Reducing CO<sub>2</sub> emissions from a gas turbine power plant by using a molten carbonate fuel cell. *Lect Notes Eng Comput Sci* 2012;3:1773–8. [http://www.iaeng.org/publication/WCE2012/WCE2012\\_pp1773-1778.pdf](http://www.iaeng.org/publication/WCE2012/WCE2012_pp1773-1778.pdf).



- [33] Ahn JH, Seop Kim T. Performance evaluation of a molten carbonate fuel cell/micro gas turbine hybrid system with oxy-combustion carbon capture. *J Eng Gas Turbines Power* 2018;140:1–11. <https://doi.org/10.1115/1.4038038>.
- [34] Ahn JH, Jeong JH, Kim TS. Performance enhancement of a molten carbonate fuel cell/micro gas turbine hybrid system with carbon capture by off-gas recirculation. *J Eng Gas Turbines Power* 2019;141:1–10. <https://doi.org/10.1115/1.4040866>.
- [35] Akrami E, Ameri M, Rocco MV. Integration of biomass-fueled power plant and MCFC-cryogenic CO<sub>2</sub> separation unit for low-carbon power production: thermodynamic and exergoeconomic comparative analysis. *Energy Convers Manag* 2020;223:113304. <https://doi.org/10.1016/j.enconman.2020.113304>.
- [36] Campanari S, Chiesa P, Manzolini G. CO<sub>2</sub> capture from combined cycles integrated with Molten Carbonate Fuel Cells. *Int J Greenh Gas Control* 2010;4:441–51. <https://doi.org/10.1016/j.ijggc.2009.11.007>.
- [37] Manzolini G, Campanari S, Chiesa P, Giannotti A, Bedont P, Parodi F. CO<sub>2</sub> separation from combined cycles using molten carbonate fuel cells. *ASME* 2012. <https://doi.org/10.1115/FuelCell2011-54719>.
- [38] Brenna M, Foidelli F, Manzolini G. Grid connection of MCFC applied to power plant with CO<sub>2</sub> capture. *Int J Electr Power Energy Syst* 2013;53:980–6. <https://doi.org/10.1016/j.ijepes.2013.06.016>.
- [39] Campanari S, Manzolini G, Chiesa P. Using MCFC for high efficiency CO<sub>2</sub> capture from natural gas combined cycles: comparison of internal and external reforming. *Appl Energy* 2013;112:772–83. <https://doi.org/10.1016/j.apenergy.2013.01.045>.
- [40] Greppi P, Bosio B, Arato E. Membranes and molten carbonate fuel cells to capture CO<sub>2</sub> and increase energy production in natural gas power plants. *Ind Eng Chem Res* 2013;52:8755–64. <https://doi.org/10.1021/ie302725a>.
- [41] Campanari S, Chiesa P, Manzolini G, Bedogni S. Economic analysis of CO<sub>2</sub> capture from natural gas combined cycles using Molten Carbonate Fuel Cells. *Appl Energy* 2014;130:562–73. <https://doi.org/10.1016/j.apenergy.2014.04.011>.
- [42] Carapellucci R, Saia R, Giordano L. Study of gas-steam combined cycle power plants integrated with MCFC for carbon dioxide capture. *Energy Proc* 2014;45:1155–64. <https://doi.org/10.1016/j.egypro.2014.01.121>.
- [43] Duan L, Zhu J, Yue L, Yang Y. Study on a gas-steam combined cycle system with CO<sub>2</sub> capture by integrating molten carbonate fuel cell. *Energy* 2014;74:417–27. <https://doi.org/10.1016/j.energy.2014.07.006>.
- [44] Spinelli M, Di Bona D, Gatti M, Martelli E, Viganò F, Consonni S. Assessing the potential of molten carbonate fuel cell-based schemes for carbon capture in natural gas-fired combined cycle power plants. *J Power Sources* 2020;448:227223. <https://doi.org/10.1016/j.jpowsour.2019.227223>.
- [45] Spallina V, Romano MC, Campanari S, Lozza G. Application of MCFC in coal gasification plants for high efficiency CO<sub>2</sub> capture. *J Eng Gas Turbines Power* 2012;134:1–8. <https://doi.org/10.1115/1.4004128>.
- [46] Duan L, Sun S, Yue L, Qu W, Yang Y. Study on a new IGCC (integrated gasification combined cycle) system with CO<sub>2</sub> capture by integrating MCFC (molten carbonate fuel cell). *Energy* 2015;87:490–503. <https://doi.org/10.1016/j.energy.2015.05.011>.
- [47] Desideri U, Proietti S, Sdringola P, Cinti G, Curbis F. MCFC-based CO<sub>2</sub> capture system for small scale CHP plants. *Int J Hydrogen Energy* 2012;37:19295–303. <https://doi.org/10.1016/j.ijhydene.2012.05.048>.
- [48] Sánchez D, Monje B, Chacartegui R, Campanari S. Potential of molten carbonate fuel cells to enhance the performance of CHP plants in sewage treatment facilities. *Int J Hydrogen Energy* 2013;38:394–405. <https://doi.org/10.1016/j.ijhydene.2012.09.145>.
- [49] Hill R, Scott S, Butler D, Sit SP, Burt D, Narayanan R, Cole T, Li C, Lightbown V, John Zhou Z. Application of molten carbonate fuel cell for CO<sub>2</sub> capture in thermal in situ oil sands facilities. *Int J Greenh Gas Control* 2015;41:276–84. <https://doi.org/10.1016/j.ijggc.2015.07.024>.
- [50] Audasso E, Bosio B, Bove D, Arato E, Barckholtz T, Kiss G, Rosen J, Elsen H, Gutierrez RB, Han L, Geary T, Willman C, Hilmi A, Yuh CY, Ghezal-Ayagh H. New, dual-anion mechanism for molten carbonate fuel cells working as carbon capture devices. *J Electrochem Soc* 2020;167:084504. <https://doi.org/10.1149/1945-7111/ab8979>.
- [51] Audasso E, Bosio B, Bove D, Arato E, Barckholtz T, Kiss G, Rosen J, Elsen H, Blanco Gutierrez R, Han L, Geary T, Willman C, Hilmi A, Yuh CY, Ghezal-Ayagh H. The effects of gas diffusion in molten carbonate fuel cells working as carbon capture devices. *J Electrochem Soc* 2020;167:114515. <https://doi.org/10.1149/1945-7111/aba8b6>.
- [52] Bove D, Audasso E, Barckholtz T, Kiss G, Rosen J, Bosio B. Process analysis of molten carbonate fuel cells in carbon capture applications. *Int J Hydrogen Energy* 2021;46:15032–45. <https://doi.org/10.1016/j.ijhydene.2020.08.020>.
- [53] Morita H, Kawase M, Mugikura Y, Asano K. Degradation mechanism of molten carbonate fuel cell based on long-term performance: long-term operation by using bench-scale cell and post-test analysis of the cell. *J Power Sources* 2010;195:6988–96. <https://doi.org/10.1016/j.jpowsour.2010.04.084>.
- [54] CEPCI. The chemical engineering plant cost index. 2022. <https://www.chemengonline.com/site/plant-cost-index/>. [Accessed 3 February 2023].
- [55] Perry R, Green D. *Perry's chemical engineers' handbook*. 7th ed.. 1997.
- [56] EBTF. European best practice guidelines for assessment of CO<sub>2</sub> capture technologies. 2011. [https://www.sintef.no/globalassets/project/decarbit/d-1-4-3\\_euro\\_bp\\_guid\\_for\\_ass\\_co2\\_cap\\_tech\\_280211.pdf](https://www.sintef.no/globalassets/project/decarbit/d-1-4-3_euro_bp_guid_for_ass_co2_cap_tech_280211.pdf). [Accessed 3 February 2023].
- [57] Turton R, Bailie RC, Whiting WB, Shaeiwitz JA. *Analysis, synthesis and design of chemical processes*. 4th ed. 2012.
- [58] FLEDGED. WP5 - Deliverable D5.1. Economic framework and simplified model for capital cost estimation. 2018. <http://www.fledged.eu/>. [Accessed 3 February 2023].
- [59] Riva L, Martinez I, Martini M, Gallucci F, van Sint Annaland M, Romano MC. Techno-economic analysis of the Ca-Cu process integrated in hydrogen plants with CO<sub>2</sub> capture. *Int J Hydrogen Energy* 2018;43:15720–38. <https://doi.org/10.1016/j.ijhydene.2018.07.002>.
- [60] NETL. Capital cost scaling methodology: revision 3 reports and prior. 2019. [https://www.netl.doe.gov/projects/files/QGESSCapitalCostScalingMethodologyRevision3ReportsandPrior\\_040119.pdf](https://www.netl.doe.gov/projects/files/QGESSCapitalCostScalingMethodologyRevision3ReportsandPrior_040119.pdf). [Accessed 3 February 2023].